Table 1 The expression of pro-inflammatory cytokines in peripheral blood mononuclear cells of HTLV-1 infected individuals

Case	Age	Sex	PVL[a]	%IFN-γ$^+$ in CD4$^+$OX40$^+$[b]	%IFN-γ$^+$ in CD4$^+$OX40$^-$	%IFN-γ$^+$ in CD4$^+$Tax$^+$[c]	%IFN-γ$^+$ in CD4$^+$Tax$^-$	% TNF-α$^+$ in CD4$^+$OX40$^+$	% TNF-α$^+$ in CD4$^+$OX40$^-$	% TNF-α$^+$ in CD4$^+$Tax$^+$	% TNF-α$^+$ in CD4$^+$Tax$^-$
HAM/TSP7	68	F	1200	56.3	8.9	74.1	12.4	66.9	26.1	70.8	25.3
HAM/TSP8	68	F	1118	77.2	5.0	91.5	4.7	84.1	10.0	87.6	10.7
HAM/TSP9	71	F	1424	64.8	4.7	80.1	5.3	70.4	18.8	80.5	16.6
mean±SE	69.0±1.0		1247±65	66.1±4.3	6.2±1.0	81.9±3.6	7.5±1.7	73.8±3.7	18.3±3.3	79.6±3.4	17.5±3.0
AC4	74	F	435	61.9	13.8	61.8	13.6	30.8	11.5	25.0	11.1
AC5	76	M	139	55.3	24.9	43.0	27.8	38.3	22.1	47.9	14.3
AC6	71	F	250	47.3	15.0	62.1	34.6	15.8	10.5	34.8	21.9
mean±SE	73.7±1.5		275±61	54.8±3.0	17.9±2.5	55.6±4.5	25.3±4.4	28.3±4.7	14.7±2.6	35.9±4.7	15.8±2.3

HAM/TSP: HTLV-1 associated myelopathy/tropical spastic paraparesis. AC: asymptomatic carrier. PVL: Proviral load.
[a] PVL: HTLV-1 tax copy number per 10^4 peripheral blood mononuclear cells (PBMCs).
[b] "%IFN-γ$^+$ in CD4$^+$OX40$^+$" means the frequency of IFN-γ$^+$ cells in the CD4$^+$OX40$^+$ cell gate.
[c] "%IFN-γ$^+$ in CD4$^+$Tax$^+$" means the frequency of IFN-γ$^+$ cells in the CD4$^+$Tax$^+$ cell gate.

Table 2 Clinical and laboratory findings of HAM/TSP patients for whom paired CSF and plasma samples were tested for soluble OX40 (sOX40)

Case	Age	Sex	Disease Duration	HTLV-1 proviral load (copies/10^4PBMCs)	HTLV-1 Ab titer (PA)	OMDS*	sOX40 (Plasma)	sOX40 (CSF)
HAM/TSP10	67	F	6 years	698	×4096	7	534.9	52.1
HAM/TSP11	29	F	1 year	1138	×16384	2	394.0	54.1
HAM/TSP12	41	F	5 years	800	×16384	4	1459.0	55.6
HAM/TSP13	62	F	1 month	224	×8192	10	626.6	752.1
HAM/TSP14	75	F	3 months	437	×4096	9	337.6	897.4
HAM/TSP15	66	F	2 months	534	×4096	9	423.5	652.5

*OMDS: Osame Motor Disability Score that graded the motor dysfunction from zero (normal walking and running) to 13 (complete bedridden): 1=normal gait but runs slow; 2=abnormal gait; 3=abnormal gait and unable to run; 4=need support while using stairs; 5=need one hand support in walking; 6=need two hands support in walking; 7=need two hands support in walking but is limited to 10 m; 8=need two hands support in walking but is limited to 5 m; 9=unable to walk but able to crawl on hands and knees; 10=crawls with hands; 11=unable to crawl but can turn sideways in bed; 12=unable to turn sideways but can move the toes.

after culture, suggesting that the anti-OX40 mAb (B-7B5) did not suppress expression of Tax but specifically eliminated OX40-positive HTLV-1 infected cells (Figure 6).

Discussion

Retroviral infection is characterized by chronic immune-system activation and pro-inflammatory cytokine production [40]. HTLV-1 infection is associated with the development of several different inflammatory conditions, including chronic arthritis, pulmonary alveolitis, polymyositis, Sjögren syndrome, and uveitis [41]. The main pathological feature of HAM/TSP is chronic inflammation of the spinal cord, characterized by perivascular cuffing of mononuclear cells accompanied by parenchymal lymphocytic infiltration. Increased spontaneous peripheral blood lymphocyte proliferation with the production of TNF-α

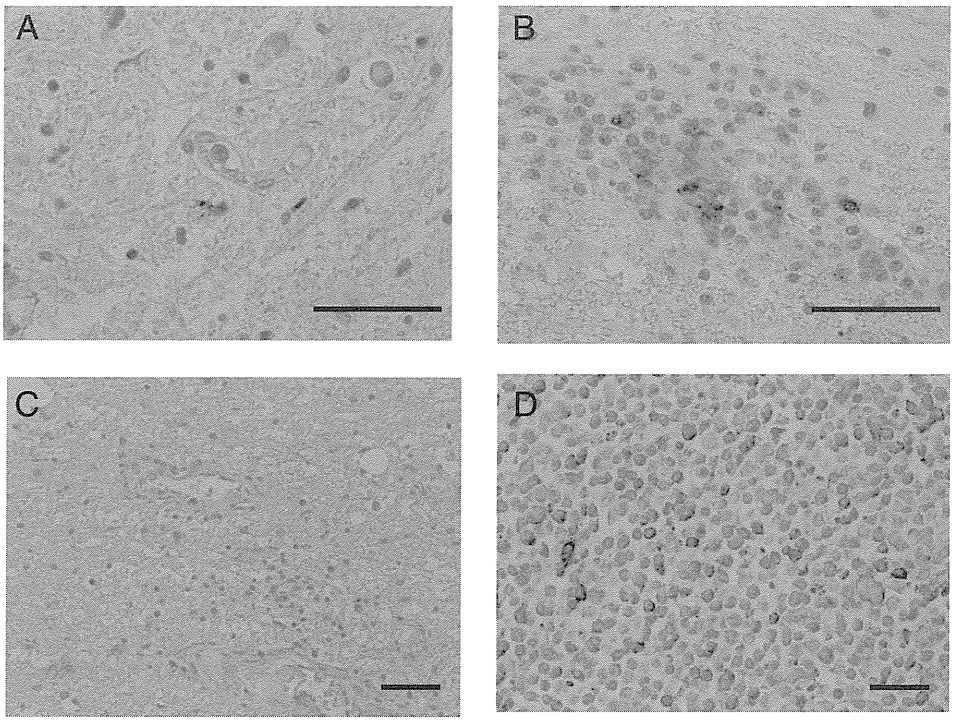

Figure 4 Expression of OX40 in inflammatory mononuclear cells in spinal cord lesions of HAM/TSP patient with short disease duration and progressive symptoms. We studied autopsy specimens from 9 HAM/TSP patients by immunohistochemical staining. **A.** No OX40 positive cells are detected in the spinal cord lesion without active inflammation of a HAM/TSP patient with a long duration of illness. Magnification: ×40. **B.** Many infiltrating mononuclear cells are positively stained by anti-OX40 mAb in the spinal cord lesion with active inflammation of HAM/TSP patient with 2.5 years of illness. Magnification: ×40. **C.** There was reduced or no OX40L protein expression in spinal cord tissues of HAM/TSP patients. OX40L showed only low background staining and there was no OX40L positive staining on inflammatory mononuclear cells in the spinal cord lesions. Magnification: ×20. **D.** Positive control staining for OX40L positive CEM-OX40L cells. Magnification: ×20. Bar: 50 μm.

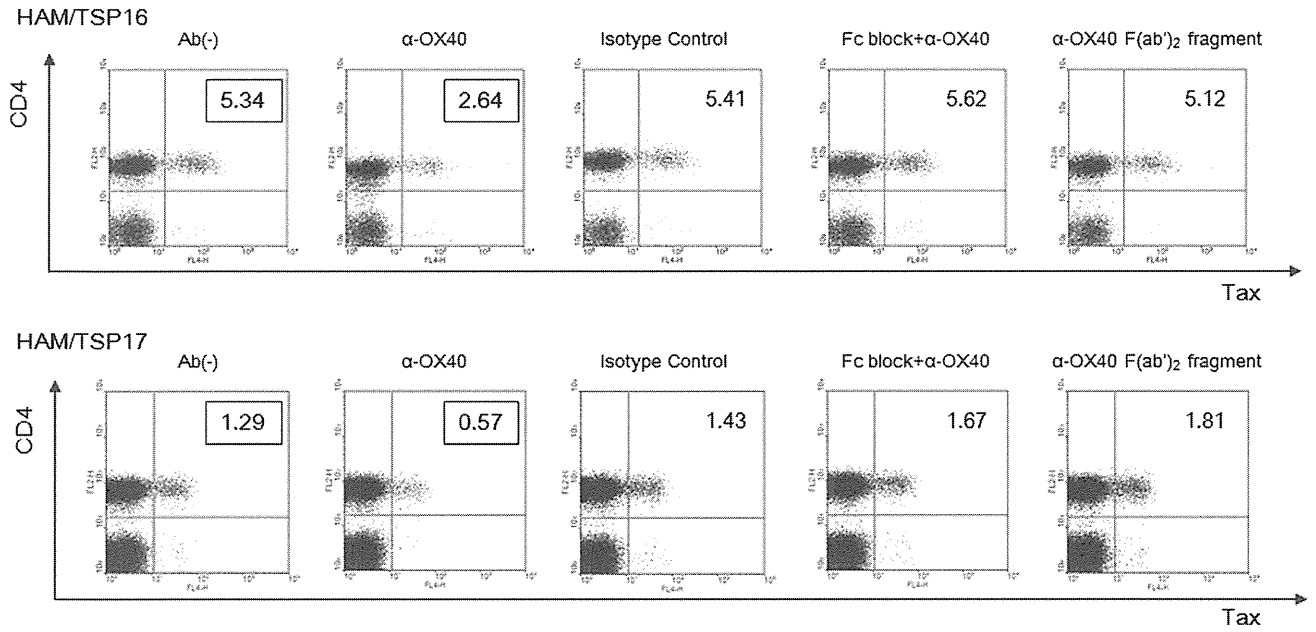

Figure 5 Anti-OX40 monoclonal antibody specifically eliminated naturally infected CD4$^+$ T cells via antibody-dependent cell-mediated cytotoxicity (ADCC) in cultured PBMCs. Anti-OX40 mAb (clone B-7B5) reduces the percentage of Tax-positive cells, whereas the isotype control mAb (clone 2C2: anti-HIV-1 gp21, mouse IgG1) has no effect on Tax expression (1st, 2nd, and 3rd panels from left). Culture of PBMCs with anti-CD16/CD32 (Fc receptor) antibody to block Fc receptors abolishes Tax suppression by anti-OX40 mAb (4th panels from left). F(ab')$_2$ fragment do not suppress Tax exppression (right panels).

and IFN-γ [42,43], high prevalence of autoantibodies, hypergammaglobulinemia, and complement fixing immune complexes have also been reported in HAM/TSP patients [6]. Recent research has shown the importance of OX40-OX40L interactions in the development of immune-mediated diseases. Specifically, a strong reduction in disease severity, or a complete lack of disease, has been reported when OX40 or OX40L is absent or neutralized in animal models. We therefore hypothesized that the OX40-positive subpopulations of chronically activated T cells exist in naturally HTLV-1-infected cells of HAM/TSP patients. These cells may function to accelerate inflammation, and blocking OX40 may have therapeutic potential in the treatment of HAM/TSP.

Previous reports indicated that OX40 is strongly stimulated by the HTLV-1 viral transactivator Tax [15,19,20]. However, these previous findings were obtained by northern blot or western blot analysis using whole cells. Thus, it was not clear if this induction occurs in naturally infected CD4$^+$ T cells of HTLV-1 infected individuals. In the present study, our flow cytometry analysis clearly showed that almost all OX40-positive cells are Tax-positive after short-term culture of naturally HTLV-1-infected cells, suggesting that OX40 is driven exclusively by Tax at the single cell level. In contrast, flow cytometry analysis of JPX-9 cells showed higher percentages of OX40$^+$Tax$^-$ cells, as well as OX40$^+$Tax$^+$ cells, after induction of Tax. Although the reasons for this discrepancy are not clear, it can be caused by differential modulation of surface and intracellular protein expression in JPX-9 cells. Our ELISA analysis indicates the existence of intracellular pools of OX40, suggesting that Tax$^+$OX40$^-$ cells also contain Tax-induced OX40 within JPX-9 cells. While the expression of another co-stimulatory member of the TNFR family, 4-1BB, has also been reported [32], our data indicate that the

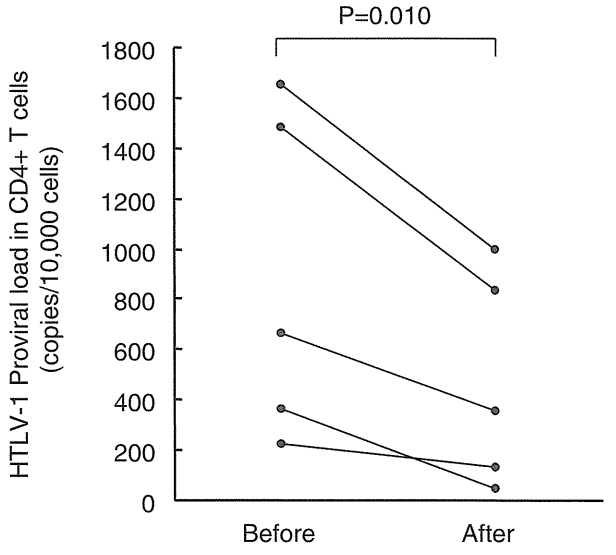

Figure 6 The HTLV-1 proviral load in CD4$^+$ T cells were significantly reduced after cultivation. CD4$^+$ T cells were isolated from PBMCs before and after cultivation, extracted genomic DNA, and measured the HTLV-1 PVL. HTLV-1 PVL in CD4+ T cells was significantly reduced after culture.

expression of OX40 was more specific than the expression of 4-1BB in Tax^+CD4^+ T cells naturally infected with HTLV-1. It has been previously reported that Tax strongly activates the 4-1BB promoter via a single NF-κB site [32] and the OX40 promoter via 2 NF-κB sites [16]; hence, sustained activation of NF-κB leads to increased expression of numerous pro-inflammatory cytokines and growth factors [44] via NF-κB signaling pathways and ultimately leads to chronic inflammation. In support of these observations, our results show that the frequencies of pro-inflammatory cytokine positive cells within the $OX40^+CD4^+$ and Tax^+CD4^+ populations from HAM/TSP patients are significantly higher than $OX40^-CD4^+$ and Tax^-CD4^+ T cells, respectively. These cells may be more likely to cross the blood brain barrier and enter the CNS, attract other cells including pro-inflammatory virus-specific $CD8^+$ cells, and result in by-stander damage to the CNS tissue.

The experimental autoimmune encephalomyelitis (EAE) rat model of human MS shows a selective upregulation of the OX40 protein in encephalitogenic myelin basic protein-specific T cells in the spinal cord during onset of the disease [21]. In contrast, T cells isolated from peripheral blood and spleen of the same animal express low levels of OX40 [21]. This is similar to our present finding, where OX40 was markedly expressed in infiltrating mononuclear cells in spinal cord lesions, but not in uncultivated PBMCs from HAM/TSP patients. Because locally produced pro-inflammatory cytokines up-regulate MHC class II molecules on astrocytes and microglia, increase presentation of CNS antigens, and exert a direct cytotoxic effect on oligodendrocytes [45], the observed expression of OX40 in inflammatory mononuclear cells in spinal cord lesions suggest a role for OX40 in inflammation and neuronal damage that occurs in the CNS of HAM/TSP patients. In the rat EAE model, selective depletion of myelin-reactive T cells, by treatment with an anti-OX40 mAb-conjugated immunotoxin, effectively suppressed disease symptoms [21]. The association of clinical progression of HAM/TSP with increased HTLV-1 PVL in individual patients [9] and the strong stimulation of OX40, together with the expression of the viral transactivator Tax in $CD4^+$ T cells, indicates that targeting of OX40 positive T cells by anti-OX40 antibodies may provide a novel therapeutic strategy for the treatment of HAM/TSP.

In the present study, an anti-OX40 monoclonal antibody specifically eliminated naturally infected $CD4^+$ T cells in cultured PBMCs via ADCC. This indicates that effector cells may actively lyse HTLV-1-infected $CD4^+$ T cells that are bound by the anti-OX40 antibody. Indeed, defucosylated humanized anti-CC chemokine receptor 4 (CCR4) mAbs, which exert a strong ADCC effect, were found to be effective and well tolerated as a treatment for patients with relapsed CCR4-positive ATL or peripheral T-cell lymphoma [46]. In the present study, OX40 expression was not observed in T cells of healthy individuals, and its expression was more specific than CCR4 for HTLV-1-infected cells. This finding suggests that specific elimination of HTLV-1-infected T cells by defucosylated humanized anti-OX40 monoclonal antibodies might be a promising future approach for treatment of HAM/TSP.

We also found that plasma sOX40 levels were more elevated in HTLV-1-infected individuals (chronic HAM/TSP patients and ACs) than in NCs. Three rapidly progressive HAM/TSP patients also showed higher levels of sOX40 in the CSF than in the plasma, suggesting the possibility that sOX40 is released at high levels following strong intrathecal immune activation. In contrast, expression of OX40L was absent in HTLV-1-infected lymphocytes even after short term ex vivo cultivation, in active-chronic spinal cord lesions of HAM/TSP patient, and in plasma of HTLV-1 infected individuals. Therefore, OX40 signals might be generated by interactions with OX40L on antigen presenting cells or endothelial cells at specialized sites such as lymphoid organs. In such lesions, similar to other members of the TNF receptor superfamily like 4-1BB, sOX40 may act as an antagonist to membrane-bound receptors and induce signaling in $OX40L^+$ cells to produce cytokines, which in turn drive specific T helper (Th)-cell differentiation and suppress the generation of adaptive Tregs to participate in HAM/TSP pathogenesis.

In conclusion, we demonstrate that OX40 was specifically expressed in $CD4^+$ T cells naturally infected with HTLV-1. These cells have the potential to produce pro-inflammatory cytokines along with the expression of the viral transactivator Tax. Higher levels of sOX40 were found in the CSF than in the plasma of three rapidly progressive HAM/TSP patients, and OX40 was overexpressed in the spinal cord infiltrating mononuclear cells of HAM/TSP patient with active disease. Anti-OX40 mAb was able to specifically eliminate HTLV-1-infected $CD4^+OX40^+Tax^+$ T cells via ADCC. These findings indicate that, in addition to its established role in the regulation of T cell division and survival, OX40 may be a key molecule in the pathogenesis of HAM/TSP, as well as a potential target for immunotherapy.

Methods

Patients

Peripheral blood was studied from 23 patients with a clinical diagnosis of HAM/TSP, 9 ACs and 13 uninfected normal controls (NCs). The diagnosis of HAM/TSP was made according to the World Health Organization diagnostic criteria [47]. In this paper, chronic HAM/TSP means typical cases fulfilling diagnostic criteria and rapidly progressive HAM/TSP is defined by patients' incapacity to walk unaided within three months after

symptoms' onset. This study was approved by the Institutional Review Board of the University of the Ryukyus with license number H21-1-9. All patients provided written informed consent for the collection of samples and subsequent analysis. The CSF and plasma samples were collected before starting therapy. Control subjects of other neurological diseases were MS (n=12), aseptic meningitis (n=8), systemic lupus erythematosus (SLE) with neurological manifestations (n=5), chronic inflammatory demyelinating polyneuropathy (CIDP) (n=9), Guillain-Barré syndrome (GBS) (n=6), and amyotrophic lateral sclerosis (ALS) (n=9). The specimens were stored at −80°C until use.

Cell culture

Six HTLV-1 infected T-cell lines (HUT-102, MT-1, MT-2, MT-4, SLB-1, C5/MJ) and two HTLV-1-uninfected T-cell lines (CEM-OX40L, CEM-OX40) were used in this study. CEM-OX40 and CEM-OX40L cell lines are stable CEM-derived cell lines expressing the human OX40 or OX40L, respectively. The Tax-inducible JPX-9 cell line is a derivative of the Jurkat HTLV-1 negative human T cell leukemia cell line, which expresses biologically active Tax protein under the control of the metallothionein promoter [29]. These cells were cultured in RPMI 1640 medium supplemented with 10% heat inactivated fetal calf serum (FCS), 50 U/ml penicillin, and 50 μg/ml streptomycin (Wako) at 37°C in 5% CO_2.

Preparation of PBMC samples

Fresh peripheral blood mononuclear cells (PBMCs) were isolated on a Histopaque-1077 (Sigma) density gradient centrifugation, washed twice in RPMI 1640 with 10% heat inactivated FCS, and stored in liquid nitrogen as stocked lymphocytes until use. $CD4^+$ T cells were isolated from PBMCs by positive immunoselection with the Dynal® CD4-positive isolation kit (Invitrogen), according to the manufacturer's protocol. In brief, PBMCs were incubated with anti-CD4-coated beads for 30 min at 4°C under gentle tilt rotation. Captured $CD4^+$ cells were collected with a magnet (Dynal MPC-S) and detached from beads with DETACHaBEAD CD4/CD8® (Invitrogen). Purity was >99% $CD4^+$ T cells, as determined by flow cytometry (data not shown). To induce cytokine production by $OX40^+CD4^+$ T cells, PBMCs were cultivated for 12 hours, then 0.1 ng/ml phorbol myristate acetate (PMA) (Sigma) and 0.5 μg/ml A23187 (Sigma) and 2 mM monensin (Sigma) were added to the culture medium and further cultivated for 5 hours.

Monoclonal antibodies and reagents

We produced the following monoclonal antibodies (mAbs) in our laboratory: mouse IgG1 mAbs anti-human OX40L (clones 5A8, 8F4), anti-human OX40 (clones B-7B5 and 17D8), anti-HIV-1 p24 (clone 2C2 and NP24), and mouse IgG3 mAb anti-HTLV-1 Tax (clone Lt-4) [48] as well as rat IgG2b mAbs anti-human OX40 (clone W4-54), anti-human OX40L (clone W18) and isotype control anti-HCV (clone MO-8). Some of these mAbs were labeled using FITC, Cy5, or HRP using commercial labeling kits (Dojin or Amersham, Japan) according to the manufacturers' instructions. Biotinylated recombinant soluble human OX40L (sOX40L in a form of murine CD8-fusion protein) was purchased from Ancell (Bayport, MN) and used with PE-streptavidin (Biolegend) for staining. Recombinant human OX40 ligand/TNFSF4 and recombinant human OX40/TNFRSF4/Fc Chimera were purchased from R&D Systems (Minneapolis, MN) and used for the standard curve in sOX40L and sOX40 ELISA, respectively.

Immunohistochemistry

Immunohistochemical staining of the spinal cord specimens from HAM/TSP patients was performed on buffered formalin-fixed paraffin-embedded sections using EnVision (DAKO) method for signal detection as described previously [36]. The clinical and pathological characteristics of the patients are described elsewhere [36-39]. The monoclonal antibodies to OX40 (clone B-7B5) and OX40L (clone 8F4) were used at a final concentration of 1 μg/ml.

Flow cytometry

Cell surface staining

After thawing, cells were washed three times with phosphate-buffered saline (PBS) and fixed in PBS containing 2% paraformaldehyde (Sigma) for 20 minutes at 4°C. Fixed cells were washed with PBS containing 7% of normal goat serum (Sigma) and then incubated for 15 minutes at room temperature with various combinations of fluorescence-conjugated mAbs as follows: phycoerythrin-cyanin 5.1 (PC5)-labeled anti-CD4 (13B8.2), PC5-labeled anti-CD8 (B9.11), phycoerythrin (PE)-labeled anti-CD4 (13B8.2) (Beckman Coulter), PE-labeled anti-4-1BB (4B4) (eBioscience), fluorescein isothiocyanate (FITC)-labeled anti-OX40 (B-7B5) and OX40L (5A8). Isotype matched mouse immunoglobulins were used as a control. After the staining procedure, the cells were washed twice and analyzed by standard flow cytometry using a FACS Calibur and Cell Quest software (BD).

Concomitant detection of intracellular and cell surface molecules

For intracellular staining of Tax and/or cytokines, surface stained cells were washed and permeabilized with PBS/7% normal goat serum containing 0.2% saponin (Sigma) (PBS-SAPO) for 10 minutes at room temperature. Permeabilized cells were then washed twice and resuspended in PBS-SAPO containing FITC or cyanin 5 (Cy5)-labeled anti-Tax

mAb (Lt-4), PE-labeled anti TNF-α (BD Pharmingen) or PE-labeled IFN-γ (BD Pharmingen) mAb for 20 minutes at room temperature. Finally, the cells were washed twice and analyzed by flow cytometry.

Flow cytometry based binding assay

To determine whether cell surface OX40 is functional, aliquots of Fc-blocked cells were incubated with biotinylated recombinant soluble OX40L at a concentration of 2.5 mg/ml for 30 min on ice, followed by staining with PE-streptavidin (Biolegend) for 30 min on ice. After the staining procedure, the cells were washed twice and analyzed by flow cytometry.

ELISA

Cell lysates were prepared by lysis of 2×10^7 cells in 1ml of a lysis buffer (10 mM Tris–HCl, pH8.0, 140 mM NaCl, 3 mM MgCls, 2 mM phenylmethylsulfonyl fluoride, 0.5% Nonidet P-40) on ice for 20 min, followed by centrifugation at 13,000 × g for 10 min at 4°C. Both OX40 and OX40L levels in cell lysates, culture supernatants, plasma and CSF were assayed by in house made sandwich ELISA using monoclonal antibodies against OX40 (clone 17D8 for capture and W4-54 for detection) and OX40L (clone 8F4 for capture and W18 for detection). Briefly, 96-well Immuno Module/Strip Plates (Nunc) was coated with either anti-OX40 monoclobal antibody (clone 17D8) or anti-OX40L monoclobal antibody (clone 8F4) at 4°C overnight, then blocked with 1% casein in 0.02% thimerosal-PBS at room temperature for 30 min. After washing plates three times with wash buffer (PBS with 0.05% Tween 20, pH 7.5), 50 μl of irrelevant mouse IgG1 (anti-HIV1 p24 mAb NP24) was added into each well as a blocking antibody. OX40 or OX40L standard was diluted to 4,000 pg/ml in dilution buffer (PBS with 0.1% BSA, 0.5% Triton X100, 0.05% Tween20), and two-fold serial dilutions were performed ranged from 4,000 to 16 pg/ml. Then 50 μl of the diluted standard or samples (cell lysates, culture supernatants, plasma and CSF) were added into 96-well plates and incubated one hour at room temparature. After washing plates three times, 50 μl each of diluted (0.2 μg/μl) anti-OX40 monoclobal antibody (clone W4-54) or anti-OX40L monoclobal antibody (clone W18) conjugated to HRP was added as detection antibody and incubated for one hour at room temperature. Color reactions using alkaline-phosphatase substrate (Sigma-Aldrich) were then evaluated by Model 680 Microplate Reader (Bio-Rad) reading at 450 nm with reference at 630 nm, and the data was analyzed using the Microplate manager III software (Bio-Rad). Results are shown as mean ± SE for duplicate wells. Human interleukin-2 soluble receptor alpha (IL-2sRα) was measured by ELISA according to the manufacturer's instruction (Quantikine Human IL-2sRα Immunoassay, R&D Systems, Inc. MN).

Genomic DNA, RNA extraction and cDNA synthesis

Genomic DNA was extracted from the frozen PBMCs by QIAamp blood kit (QIAGEN, Tokyo, Japan). RNA from 1×10^5 enriched $CD4^+$ T cells was extracted using RNeasy Mini Kit with on-column DNase digestion (QIAGEN, Tokyo, Japan) according to the manufacturer's instructions. Complementary DNA (cDNA) was synthesized using PrimeScript® RT reagent Kit (Takara, Kyoto, Japan). All reaction procedures were performed as suggested by the manufacturer.

Quantification of HTLV-1 proviral load and anti-HTLV-1 antibody titers

To examine the HTLV-1 PVL, we carried out a quantitative PCR method using Thermal Cycler Dice® Real Time System (Takara, Japan) with 100 ng of genomic DNA (roughly equivalent to 10^4 cells) from PBMCs samples as reported previously [8]. Based on the standard curve created by four known concentrations of template, the concentration of unknown samples were determined. Using β-actin as an internal control, the amount of HTLV-1 proviral DNA was calculated by the following formula: copy number of HTLV-1 tax per 1×10^4PBMCs = [(*copy number of tax*)/(*copy number of β – actin*/2)] × 10^4. All samples were performed in triplicate. Serum HTLV-1 antibody titers were determined by a particle agglutination method (Serodia-HTLV-1®, Fujirebio, Japan).

Real-Time RT-PCR analysis

We used the real-time RT-PCR method to carry out a quantitative analysis of the expression of the tax and OX40 mRNA by using Thermal Cycler Dice® Real Time System (Takara, Japan) as reported previously [49]. HTLV-1 tax or OX40 mRNA load was calculated by the following formula: HTLV - 1 tax mRNA load = value of tax/value of HPRT (Hypoxanthine Phosphorisbosytransferase). OX40 mRNA load = value of OX40/value of HPRT. We used aliquots of the same standard MT-2 cDNA preparation for all assays and the correlation values of standard curves were always more than 99%. The sequences of primers for tax mRNA detection were as follows: 5′- ATC CCG TGG AGA CTC CTC AA-3′ and 5′- ATC CCG TGG AGA CTC CTC AA-3′, and the probe that surrounded the splice junction site of tax mRNA was 5′- TCC AAC ACC ATG GCC CAC TTC CC-3′. The sequences of primers for OX40 mRNA detection were as follows: 5′-AAC CAG GCC TGC AAG CCC T-3′ and 5′-GTC CCT GTC CTC ACA GAT T-3′, and the probe that span the junction between exon 4 and 5 was 5′- ACC AAC TGC ACC TTG GCT GGG AAG CA-3′. We used the HPRT primers and probe set (Applied Biosystems) for internal calibration. All assays were performed in triplicate.

Statistical analysis

To test for significant differences among the cell populations between three different groups of subjects (HAM/TSP, ACs and NCs), the Kruskal-Wallis test was employed. For multiple comparisons, we used Sheffe's F to analyze statistical difference. Correlations between variables were examined by Spearman rank correlation analysis. We made paired comparison of changes in HTLV-1 PVL in $CD4^+$ T cells before and after PBMCs cultivation by using a paired t-test. The results represent the mean ± SE where applicable. Values of $p<0.05$ were considered statistically significant.

Additional files

Additional file 1: Figure S1. OX40 was expressed on the surface of Tax^+ $CD4^+$ T cells from HTLV-1 infected individuals. OX40 was detected on $CD4^+$ T cells of HAM/TSP patients (HAM/TSP3, 4) and AC (AC1) with anti-OX40 mAb (clones B-7B5) after 16 hours in vitro cultivation in the absence of any growth factors or mitogen (center panels). OX40 was expressed almost exclusively in naturally infected $CD4^+$ T cells that also expressed Tax (right panels). **FigureS2.** The expression of 4-1BB on $CD4^+$ T cells from HAM/TSP patients. **A**. 4-1BB was detected on both $CD4^+$ and CD4- T cells of HAM/TSP patients with anti-4-1BB mAb (clone 4B4, eBioscience) after 16 hours in vitro cultivation in the absence of any growth factors or mitogen. **B**. Tax protein was detected in $CD4^+$ T cells after 16 hours in vitro cultivation. **C**. The expression of 4-1BB was associated with the expression of Tax. **Figure S3.** Functional OX40 is specifically expressed on the surface of T cells naturally infected with HTLV-1. To determine if cell surface OX40 is functional, flow cytometry based binding assays have been carried out. Aliquots of Fc-blocked cells were incubated with biotinylated recombinant soluble OX40L at a concentration of 2.5 mg/ml for 30 min on ice. Then cells were washed and stained with PE-streptavidin (Biolegend) and PC5-labeled anti-CD4 for 30 min on ice. After washing, the cells were fixed and processed to detect concomitantly Tax (see Methods). The frequency of $CD4^+$ T cells that were positively stained with biotinylated recombinant soluble OX40L and PE-streptavidin was similar to the percentage of $CD4^+$ T cells stained by anti-OX40 mAb, indicating that these cells expressed functional OX40.

Additional file 2: Table S1. Ex vivo frequency of OX40 and Tax positive T cells in peripheral blood mononuclear cells from HTLV-1 infected individuals.

Abbreviations

HTLV-1: Human T-cell leukemia virus type-1; ATL: Adult T-cell leukemia; HAM/TSP: HTLV-1-associated myelopathy/tropical spastic paraparesis; ACs: Asymptomatic carriers; NCs: Normal uninfected healthy controls; MS: Multiple sclerosis; CSF: Cerebrospinal fluid; OINDs: Other inflammatory neurological diseases; ADCC: Antibody-dependent cellular cytotoxicity; PVL: Proviral load; CNS: Central nervous system; SLE: Systemic lupus erythematosus; CIDP: Chronic inflammatory demyelinating polyneuropathy; GBS: Guillain-Barré syndrome; ALS: Amyotrophic lateral sclerosis; HPRT: Hypoxanthine phosphoribosyltransferase.

Competing interests

The authors declare that they have no competing interests.

Authors' contributions

MS designed and performed the experiments, analyzed the data, and wrote the paper; TM, SI, TT, YO, and HT provided clinical samples and assembled clinical database; RT, SA, FU, and SI performed experiments, analyzed and interpreted data; YT made contribution to the conception and design of the study. All authors read and approved the final manuscript.

Acknowledgements

This study was supported by grant 21590512 and 24590556 from the Japan Society for the Promotion of Science (JSPS), the Research Grant on Intractable Disease (H22-013 and H23-126) form the Ministry of Health, Labour and Welfare of Japan, and the Novartis Foundation (Japan) for the Promotion of Science.

Author details

[1]Department of Immunology, Graduate School of Medicine, University of the Ryukyus, 207 Uehara, Okinawa 903-0215, Japan. [2]Division of Molecular Pathology, Center for Chronic Viral Diseases, Kagoshima University Graduate School of Medical and Dental Sciences, 8-35-1 Sakuragaoka, Kagoshima 890-8520, Japan. [3]Department of Neurology and Geriatrics, Kagoshima University Graduate School of Medical and Dental Sciences, 8-35-1 Sakuragaoka, Kagoshima 890-8520, Japan. [4]Department of Cardiovascular Medicine, Nephrology and Neurology, Graduate School of Medicine, University of the Ryukyus, 207 Uehara, Okinawa 903-0215, Japan. [5]Department of Neurology, Nanpu Hospital, 14-3 Nagata-cho, Kagoshima 892-8512, Japan. [6]Present Address: Department of Microbiology, Kawasaki Medical School, 577 Matsushima, Kurashiki 701-0192, Japan.

Received: 4 December 2012 Accepted: 30 April 2013
Published: 7 May 2013

References

1. Yoshida M, Seiki M, Yamaguchi K, Takatsuki K: **Monoclonal integration of human T-cell leukemia provirus in all primary tumors of adult T-cell leukemia suggests causative role of human T-cell leukemia virus in the disease.** *Proc Natl Acad Sci USA* 1984, **81**:2534–2537.
2. Hinuma Y, Nagata K, Hanaoka M, Nakai M, Matsumoto T, Kinoshita KI, Shirakawa S, Miyoshi I: **Adult T-cell leukemia: antigen in an ATL cell line and detection of antibodies to the antigen in human sera.** *Proc Natl Acad Sci USA* 1981, **78**:6476–6480.
3. Osame M, Usuku K, Izumo S, Ijichi N, Amitani H, Igata A, Matsumoto M, Tara M: **HTLV-I associated myelopathy, a new clinical entity.** *Lancet* 1986, **1**:1031–1032.
4. Gessain A, Barin F, Vernant JC, Gout O, Maurs L, Calender A, de The G: **Antibodies to human T-lymphotropic virus type-I in patients with tropical spastic paraparesis.** *Lancet* 1985, **2**:407–410.
5. Nakagawa M, Nakahara K, Maruyama Y, Kawabata M, Higuchi I, Kubota H, Izumo S, Arimura K, Osame M: **Therapeutic trials in 200 patients with HTLV-I-associated myelopathy/ tropical spastic paraparesis.** *J Neurovirol* 1996, **2**:345–355.
6. Nakagawa M, Izumo S, Ijichi S, Kubota H, Arimura K, Kawabata M, Osame M: **HTLV-I-associated myelopathy: analysis of 213 patients based on clinical features and laboratory findings.** *J Neurovirol* 1995, **1**:50–61.
7. Izumo S, Umehara F, Osame M: **HTLV-I-associated myelopathy.** *Neuropathology* 2000, **20**(Suppl):S65–68.
8. Nagai M, Usuku K, Matsumoto W, Kodama D, Takenouchi N, Moritoyo T, Hashiguchi S, Ichinose M, Bangham CR, Izumo S, Osame M: **Analysis of HTLV-I proviral load in 202 HAM/TSP patients and 243 asymptomatic HTLV-I carriers: high proviral load strongly predisposes to HAM/TSP.** *J Neurovirol* 1998, **4**:586–593.
9. Takenouchi N, Yamano Y, Usuku K, Osame M, Izumo S: **Usefulness of proviral load measurement for monitoring of disease activity in individual patients with human T-lymphotropic virus type I-associated myelopathy/tropical spastic paraparesis.** *J Neurovirol* 2003, **9**:29–35.
10. Nomoto M, Utatsu Y, Soejima Y, Osame M: **Neopterin in cerebrospinal fluid: a useful marker for diagnosis of HTLV-I-associated myelopathy/ tropical spastic paraparesis.** *Neurology* 1991, **41**:457.
11. Jacobson S: **Immunopathogenesis of human T cell lymphotropic virus type I-associated neurologic disease.** *J Infect Dis* 2002, **186**(Suppl 2):S187–192.
12. Kitze B, Usuku K, Yashiki S, Ijichi S, Fujiyoshi T, Nakamura M, Izumo S, Osame M, Sonoda S: **Intrathecal humoral immune response in HAM/TSP in relation to HLA haplotype analysis.** *Acta Neurol Scand* 1996, **94**:287–293.
13. Tattermusch S, Skinner JA, Chaussabel D, Banchereau J, Berry MP, McNab FW, O'Garra A, Taylor GP, Bangham CR: **Systems biology approaches reveal a specific interferon-inducible signature in HTLV-1 associated myelopathy.** *PLoS Pathog* 2012, **8**:e1002480.
14. Croft M: **Control of immunity by the TNFR-related molecule OX40 (CD134).** *Annu Rev Immunol* 2010, **28**:57–78.

15. Higashimura N, Takasawa N, Tanaka Y, Nakamura M, Sugamura K: **Induction of OX40, a receptor of gp34, on T cells by trans-acting transcriptional activator, Tax, of human T-cell leukemia virus type I.** *Jpn J Cancer Res* 1996, **87**:227–231.
16. Pankow R, Durkop H, Latza U, Krause H, Kunzendorf U, Pohl T, Bulfone-Paus S: **The HTLV-I tax protein transcriptionally modulates OX40 antigen expression.** *J Immunol* 2000, **165**:263–270.
17. Tanaka Y, Inoi T, Tozawa H, Yamamoto N, Hinuma Y: **A glycoprotein antigen detected with new monoclonal antibodies on the surface of human lymphocytes infected with human T-cell leukemia virus type-I (HTLV-I).** *Int J Cancer* 1985, **36**:549–555.
18. Baum PR, Gayle RB 3rd, Ramsdell F, Srinivasan S, Sorensen RA, Watson ML, Seldin MF, Baker E, Sutherland GR, Clifford KN, *et al*: **Molecular characterization of murine and human OX40/OX40 ligand systems: identification of a human OX40 ligand as the HTLV-1-regulated protein gp34.** *EMBO J* 1994, **13**:3992–4001.
19. Imura A, Hori T, Imada K, Kawamata S, Tanaka Y, Imamura S, Uchiyama T: **OX40 expressed on fresh leukemic cells from adult T-cell leukemia patients mediates cell adhesion to vascular endothelial cells: implication for the possible involvement of OX40 in leukemic cell infiltration.** *Blood* 1997, **89**:2951–2958.
20. Imura A, Hori T, Imada K, Ishikawa T, Tanaka Y, Maeda M, Imamura S, Uchiyama T: **The human OX40/gp34 system directly mediates adhesion of activated T cells to vascular endothelial cells.** *J Exp Med* 1996, **183**:2185–2195.
21. Weinberg AD, Bourdette DN, Sullivan TJ, Lemon M, Wallin JJ, Maziarz R, Davey M, Palida F, Godfrey W, Engleman E, *et al*: **Selective depletion of myelin-reactive T cells with the anti-OX-40 antibody ameliorates autoimmune encephalomyelitis.** *Nat Med* 1996, **2**:183–189.
22. Salek-Ardakani S, Song J, Halteman BS, Jember AG, Akiba H, Yagita H, Croft M: **OX40 (CD134) controls memory T helper 2 cells that drive lung inflammation.** *J Exp Med* 2003, **198**:315–324.
23. Higgins LM, McDonald SA, Whittle N, Crockett N, Shields JG, MacDonald TT: **Regulation of T cell activation in vitro and in vivo by targeting the OX40-OX40 ligand interaction: amelioration of ongoing inflammatory bowel disease with an OX40-IgG fusion protein, but not with an OX40 ligand-IgG fusion protein.** *J Immunol* 1999, **162**:486–493.
24. Pakala SV, Bansal-Pakala P, Halteman BS, Croft M: **Prevention of diabetes in NOD mice at a late stage by targeting OX40/OX40 ligand interactions.** *Eur J Immunol* 2004, **34**:3039–3046.
25. Yoshioka T, Nakajima A, Akiba H, Ishiwata T, Asano G, Yoshino S, Yagita H, Okumura K: **Contribution of OX40/OX40 ligand interaction to the pathogenesis of rheumatoid arthritis.** *Eur J Immunol* 2000, **30**:2815–2823.
26. van Wanrooij EJ, van Puijvelde GH, de Vos P, Yagita H, van Berkel TJ, Kuiper J: **Interruption of the Tnfrsf4/Tnfsf4 (OX40/OX40L) pathway attenuates atherogenesis in low-density lipoprotein receptor-deficient mice.** *Arterioscler Thromb Vasc Biol* 2007, **27**:204–210.
27. Tsukada N, Akiba H, Kobata T, Aizawa Y, Yagita H, Okumura K: **Blockade of CD134 (OX40)-CD134L interaction ameliorates lethal acute graft-versus-host disease in a murine model of allogeneic bone marrow transplantation.** *Blood* 2000, **95**:2434–2439.
28. Curry AJ, Chikwe J, Smith XG, Cai M, Schwarz H, Bradley JA, Bolton EM: **OX40 (CD134) blockade inhibits the co-stimulatory cascade and promotes heart allograft survival.** *Transplantation* 2004, **78**:807–814.
29. Nagata K, Ohtani K, Nakamura M, Sugamura K: **Activation of endogenous c-fos proto-oncogene expression by human T-cell leukemia virus type I-encoded p40tax protein in the human T-cell line, Jurkat.** *J Virol* 1989, **63**:3220–3226.
30. Taylor L, Schwarz H: **Identification of a soluble OX40 isoform: development of a specific and quantitative immunoassay.** *J Immunol Methods* 2001, **255**:67–72.
31. Komura K, Yoshizaki A, Kodera M, Iwata Y, Ogawa F, Shimizu K, Wayaku T, Yukami T, Murata M, Hasegawa M, *et al*: **Increased serum soluble OX40 in patients with systemic sclerosis.** *J Rheumatol* 2008, **35**:2359–2362.
32. Pichler K, Kattan T, Gentzsch J, Kress AK, Taylor GP, Bangham CR, Grassmann R: **Strong induction of 4-1BB, a growth and survival promoting costimulatory receptor, in HTLV-1-infected cultured and patients' T cells by the viral Tax oncoprotein.** *Blood* 2008, **111**:4741–4751.
33. Ijichi S, Izumo S, Eiraku N, Machigashira K, Kubota R, Nagai M, Ikegami N, Kashio N, Umehara F, Maruyama I, *et al*: **An autoaggressive process against bystander tissues in HTLV-I-infected individuals: a possible pathomechanism of HAM/TSP.** *Med Hypotheses* 1993, **41**:542–547.
34. Daenke S, Bangham CR: **Do T cells cause HTLV-1-associated disease?: a taxing problem.** *Clin Exp Immunol* 1994, **96**:179–181.
35. Umehara F, Nakamura A, Izumo S, Kubota R, Ijichi S, Kashio N, Hashimoto K, Usuku K, Sato E, Osame M: **Apoptosis of T lymphocytes in the spinal cord lesions in HTLV-I-associated myelopathy: a possible mechanism to control viral infection in the central nervous system.** *J Neuropathol Exp Neurol* 1994, **53**:617–624.
36. Umehara F, Izumo S, Nakagawa M, Ronquillo AT, Takahashi K, Matsumuro K, Sato E, Osame M: **Immunocytochemical analysis of the cellular infiltrate in the spinal cord lesions in HTLV-I-associated myelopathy.** *J Neuropathol Exp Neurol* 1993, **52**:424–430.
37. Umehara F, Izumo S, Ronquillo AT, Matsumuro K, Sato E, Osame M: **Cytokine expression in the spinal cord lesions in HTLV-I-associated myelopathy.** *J Neuropathol Exp Neurol* 1994, **53**:72–77.
38. Moritoyo T, Reinhart TA, Moritoyo H, Sato E, Izumo S, Osame M, Haase AT: **Human T-lymphotropic virus type I-associated myelopathy and tax gene expression in CD4+ T lymphocytes.** *Ann Neurol* 1996, **40**:84–90.
39. Umehara F, Okada Y, Fujimoto N, Abe M, Izumo S, Osame M: **Expression of matrix metalloproteinases and tissue inhibitors of metalloproteinases in HTLV-I-associated myelopathy.** *J Neuropathol Exp Neurol* 1998, **57**:839–849.
40. Copeland KF, Heeney JL: **T helper cell activation and human retroviral pathogenesis.** *Microbiol Rev* 1996, **60**:722–742.
41. Uchiyama T: **Human T cell leukemia virus type I (HTLV-I) and human diseases.** *Annu Rev Immunol* 1997, **15**:15–37.
42. Itoyama Y, Minato S, Kira J, Goto I, Sato H, Okochi K, Yamamoto N: **Spontaneous proliferation of peripheral blood lymphocytes increased in patients with HTLV-I-associated myelopathy.** *Neurology* 1988, **38**:1302–1307.
43. Nakamura T, Nishiura Y, Ichinose K, Shirabe S, Tsujino A, Goto H, Furuya T, Nagataki S: **Spontaneous proliferation of and cytokine production by T cells adherent to human endothelial cells in patients with human T-lymphotropic virus type I-associated myelopathy.** *Intern Med* 1996, **35**:195–199.
44. Li Q, Verma IM: **NF-kappaB regulation in the immune system.** *Nat Rev Immunol* 2002, **2**:725–734.
45. Vartanian T, Li Y, Zhao M, Stefansson K: **Interferon-gamma-induced oligodendrocyte cell death: implications for the pathogenesis of multiple sclerosis.** *Mol Med* 1995, **1**:732–743.
46. Yamamoto K, Utsunomiya A, Tobinai K, Tsukasaki K, Uike N, Uozumi K, Yamaguchi K, Yamada Y, Hanada S, Tamura K, *et al*: **Phase I study of KW-0761, a defucosylated humanized anti-CCR4 antibody, in relapsed patients with adult T-cell leukemia-lymphoma and peripheral T-cell lymphoma.** *J Clin Oncol* 2010, **28**:1591–1598.
47. Osame M: *Review of WHO Kagoshima meeting and diagnostic guidelines for HAM/TSP.* New York: Raven Press; 1990.
48. Lee B, Tanaka Y, Tozawa H: **Monoclonal antibody defining tax protein of human T-cell leukemia virus type-I.** *Tohoku J Exp Med* 1989, **157**:1–11.
49. Saito M, Matsuzaki T, Satou Y, Yasunaga J, Saito K, Arimura K, Matsuoka M, Ohara Y: **In vivo expression of the HBZ gene of HTLV-1 correlates with proviral load, inflammatory markers and disease severity in HTLV-1 associated myelopathy/tropical spastic paraparesis (HAM/TSP).** *Retrovirology* 2009, **6**:19.

doi:10.1186/1742-4690-10-51
Cite this article as: Saito *et al.*: Increased expression of OX40 is associated with progressive disease in patients with HTLV-1-associated myelopathy/tropical spastic paraparesis. *Retrovirology* 2013 **10**:51.

Genome-wide Determinants of Proviral Targeting, Clonal Abundance and Expression in Natural HTLV-1 Infection

Anat Melamed[1], Daniel J. Laydon[1], Nicolas A. Gillet[1,2], Yuetsu Tanaka[3], Graham P. Taylor[4], Charles R. M. Bangham[1]*

1 Department of Immunology, Wright-Fleming Institute, Imperial College London, London, United Kingdom, **2** Molecular and Cellular Epigenetics, Interdisciplinary Cluster for Applied Genoproteomics (GIGA) of University of Liège (ULg), Liège, Belgium, **3** Graduate School and Faculty of Medicine, University of the Ryukyus, Okinawa, Japan, **4** Department of Genitourinary Medicine and Communicable Diseases, Wright-Fleming Institute, Imperial College London, London, United Kingdom

Abstract

The regulation of proviral latency is a central problem in retrovirology. We postulate that the genomic integration site of human T lymphotropic virus type 1 (HTLV-1) determines the pattern of expression of the provirus, which in turn determines the abundance and pathogenic potential of infected T cell clones in vivo. We recently developed a high-throughput method for the genome-wide amplification, identification and quantification of proviral integration sites. Here, we used this protocol to test two hypotheses. First, that binding sites for transcription factors and chromatin remodelling factors in the genome flanking the proviral integration site of HTLV-1 are associated with integration targeting, spontaneous proviral expression, and in vivo clonal abundance. Second, that the transcriptional orientation of the HTLV-1 provirus relative to that of the nearest host gene determines spontaneous proviral expression and in vivo clonal abundance. Integration targeting was strongly associated with the presence of a binding site for specific host transcription factors, especially STAT1 and p53. The presence of the chromatin remodelling factors BRG1 and INI1 and certain host transcription factors either upstream or downstream of the provirus was associated respectively with silencing or spontaneous expression of the provirus. Cells expressing HTLV-1 Tax protein were significantly more frequent in clones of low abundance in vivo. We conclude that transcriptional interference and chromatin remodelling are critical determinants of proviral latency in natural HTLV-1 infection.

Citation: Melamed A, Laydon DJ, Gillet NA, Tanaka Y, Taylor GP, et al. (2013) Genome-wide Determinants of Proviral Targeting, Clonal Abundance and Expression in Natural HTLV-1 Infection. PLoS Pathog 9(3): e1003271. doi:10.1371/journal.ppat.1003271

Editor: Michael Emerman, Fred Hutchinson Cancer Research Center, United States of America

Received November 6, 2012; **Accepted** February 10, 2013; **Published** March 21, 2013

Funding: This project was supported by the Wellcome Trust (www.wellcome.ac.uk/), grant number P08165. We are grateful for support from the Imperial NIHR Biomedical Research Centre funding scheme. The funders had no role in study design, data collection and analysis, decision to publish, or preparation of the manuscript.

Competing Interests: The authors have declared that no competing interests exist.

* E-mail: c.bangham@imperial.ac.uk

Introduction

It is poorly understood how the flanking host genome influences transcription of an integrated provirus. Experiments on artificially modified proviral reporter constructs have yielded contradictory evidence on the role of flanking host promoters in either driving proviral transcription, or suppressing it by transcriptional interference [1,2]. Conclusions from experiments on single artificial clones therefore cannot be reliably generalized: evidence is required from genome-wide studies of integrated proviruses in natural infection.

Human T lymphotropic virus Type 1 (HTLV-1) persists in vivo by two routes: by driving selective clonal proliferation of infected T lymphocytes ('mitotic spread') and by de novo infection ('infectious spread') via the virological synapse [3]. HTLV-1 replication is counterbalanced by a strong, chronically activated cytotoxic T lymphocyte (CTL) immune response [4]. The HTLV-1 proviral load (number of proviral copies per 100 PBMCs) varies between infected individuals by over 1000-fold. The proviral load is the strongest correlate of HTLV-1 associated diseases, in particular Adult T-cell Leukemia-Lymphoma (ATLL, [5]) and HTLV-1 Associated Myelopathy/Tropical Spastic Paraparesis (HAM/TSP, [6]).

Mitotic spread of HTLV-1 results in expanded clones of cells that carry the provirus in the same genomic integration site [7]. Infectious spread results in integration of the provirus at a new genomic position. We have recently shown that the majority of naturally infected T-cell clones carry a single proviral copy [8]. Integration of HTLV-1 does not favour specific hotspots, but is more frequent in transcriptionally active areas of the genome [9,10,11]. However, the factors that determine integration targeting and the abundance and expression of the HTLV-1 provirus in vivo are unknown. Two HTLV-1 gene products are thought to play a crucial role in viral persistence in vivo. Tax, the transcriptional transactivator of the virus, elicits abundant, chronically activated CTLs [12,13,14], indicating continuous or repeated expression of Tax in vivo. Ex vivo, Tax protein is spontaneously expressed in a fraction of infected peripheral blood mononuclear cells (PBMCs) after overnight culture [15]. *HBZ* is the only gene expressed from the minus strand of the provirus. *HBZ* also promotes infected cell proliferation [16] and the CTL response to HBZ protein is a key determinant of proviral load and the risk of the inflammatory disease HAM/TSP [17,18]. Tax enhances HBZ expression; HBZ protein exerts negative feedback on Tax expression [19,20].

Author Summary

HTLV-1 is a human retrovirus, estimated to infect over 10 million individuals worldwide, which causes the inflammatory disease HTLV-1-associated Myelopathy/Tropical Spastic Paraparesis and an aggressive malignancy known as Adult T-cell Leukemia/Lymphoma. The mechanisms that allow the virus to maintain a life-long infection are not fully understood. Here we identified attributes of the host genome flanking the integrated HTLV-1 provirus associated with integration targeting and spontaneous expression of the provirus in vitro, and clonal expansion in vivo. Spontaneous expression (after short-term culture) of the viral protein Tax, which is known to drive proliferation of the infected cell, was significantly more frequent among less expanded clones, suggesting that Tax-expressing clones are more efficiently controlled by the immune response. Certain transcription start sites immediately upstream of the viral integration site were associated with virus latency, which in turn was associated with clonal expansion in vivo.

We hypothesize that the genomic integration site of HTLV-1 determines the pattern and intensity of expression of the plus and minus proviral strands, which in turn determine the equilibrium abundance and the pathogenic potential of an infected T cell clone in vivo. To test this hypothesis, we used our recently described protocol [11] of high-throughput mapping and quantification of proviral integration sites in fresh primary PBMCs from HTLV-1-infected individuals.

Results

HTLV-1 preferentially integrates within 1 kb of a host transcription start site and is strongly biased to specific transcription factor binding sites

To identify genomic factors associated with the targeting of HTLV-1 integration, we infected Jurkat T cells by short co-culture with the HTLV-1-producing cell line MT2. The integration sites were then analysed using our high-throughput protocol and compared to a control list of random sites in the human genome. Figure 1A illustrates the possible orientations (same or opposite) of the nearby genomic features, such as transcription start sites, either upstream or downstream of the integrated provirus.

We previously showed [11] that 47% of de novo HTLV-1 proviral integration events lie within a RefSeq gene. This frequency is slightly higher than expected by chance, but is much lower than that observed for HIV (~70%), which uses the host protein LEDGF to target proviral integration to genes [21]. As expected by chance, ~50% of proviruses integrated within host genes were in the same transcriptional orientation as the host gene (Figure 1D, in vitro).

Gillet et al [11] reported a significantly higher than expected proportion of in vitro integration sites within 10 kb of a RefSeq gene. We extended this analysis to identify the optimal (most frequent) distance between the integration site and the nearest host transcription start site (TSS). The results (Figure 1B) show a peak preference (measured by the odds ratio, OR, observed/expected) towards integration in proximity to TSS at ~1 kb of the integrated provirus (upstream or downstream); the OR gradually diminished until it reached 1 (same as random expectation) at ~1 Mb from the integration site (Figure 1B). There was a small bias (non-significant for in vitro integration) towards integration with a TSS downstream of the integration site (Figure 1C, in vitro).

Similarly, we observed a bias (up to 2-fold greater than random) towards integration in proximity to CpG islands; again, the bias reached a peak at 1 kb from the nearest CpG island (supplementary Figure S4).

We showed previously [11] that HTLV-1 provirus preferentially integrates in transcriptionally active regions of the host genome. To test the hypothesis that specific transcription factor binding sites (TFBS) influence HTLV-1 proviral targeting, expression and clonal abundance, we used data on genome-wide TFBS ChIP-seq: where available, from primary $CD4^+$ T cells; otherwise, from T cells or other human cell types; see Table S3 for complete listing of the datasets used.

In vitro integration sites showed a remarkably strong bias (compared with random sites) towards integration in proximity to specific TFBS, in particular STAT1, p53, HDACs (e.g. HDAC3, HDAC6) and HATs (e.g. p300, CBP) (Table S3). In most cases the effect was localized to within 100–1000 bases of the integration site (Figure 2A) and declined sharply at greater distances. Two patterns were observed in this biased integration. First, the preference towards integration in proximity to TFBS was typically symmetrical (e.g. p300), i.e. equally strong upstream and downstream of the integration site but in some cases was asymmetrical (e.g. STAT1), with a bias towards one side (often downstream). Second, in many cases we observed a sharp decrease in the preferential integration at 10 bases from the TFBS, such as STAT1 Figure 2A). This pattern was consistently observed across several in vitro and in vivo datasets (supplementary Figures S1, S2).

Because certain TFBS are frequently co-located in the human genome [22], we wished to test which TFBS were independently associated with targeting of the integration site. First, a likelihood ratio test was used to test whether the TFBS was selectively associated with integration either upstream or downstream of the integration site, and each TFBS was then tested individually using a univariate model. We then combined all significant factors using a step-down multivariate logistic regression analysis until only independently significant ($p<0.05$) factors remained. Most factors that were independently associated with integration site targeting occurred with equal frequency upstream or downstream of the integration site (Figure 2B, see also supplementary Table S7). The factors with the highest odds ratios were the transcription factor p53 and the histone deacetylase HDAC6.

Effect of HTLV-1 integration sites on clonal expansion

We previously reported [11] a significant association between certain features in the flanking genome and in vivo expansion of the infected T-cell clone. Here, we found that proviruses integrated within a gene were more frequent in larger (more abundant) clones than in smaller clones in vivo, but only when the provirus was integrated in the same transcriptional orientation as the host gene (Figure 1D); the frequency of integration in the opposite orientation was not positively correlated with clonal abundance.

High clone abundance (Figure 1C, top two bins) was associated with the presence of a host TSS within 1 kb downstream of the provirus; here, the transcriptional orientation of the provirus had less effect on abundance than in the case of proviruses integrated within a host gene. The excess frequency of TSS downstream (but not upstream) was much higher in integration sites in vivo than in vitro, in particular when the provirus was integrated in the same orientation as the nearby host gene (p(same) $<10^{-5}$; p(opposite) <0.05, χ^2 test). The presence of a host CpG island within 1 kb downstream was also selectively associated with clone high abundance (Figure 1E).

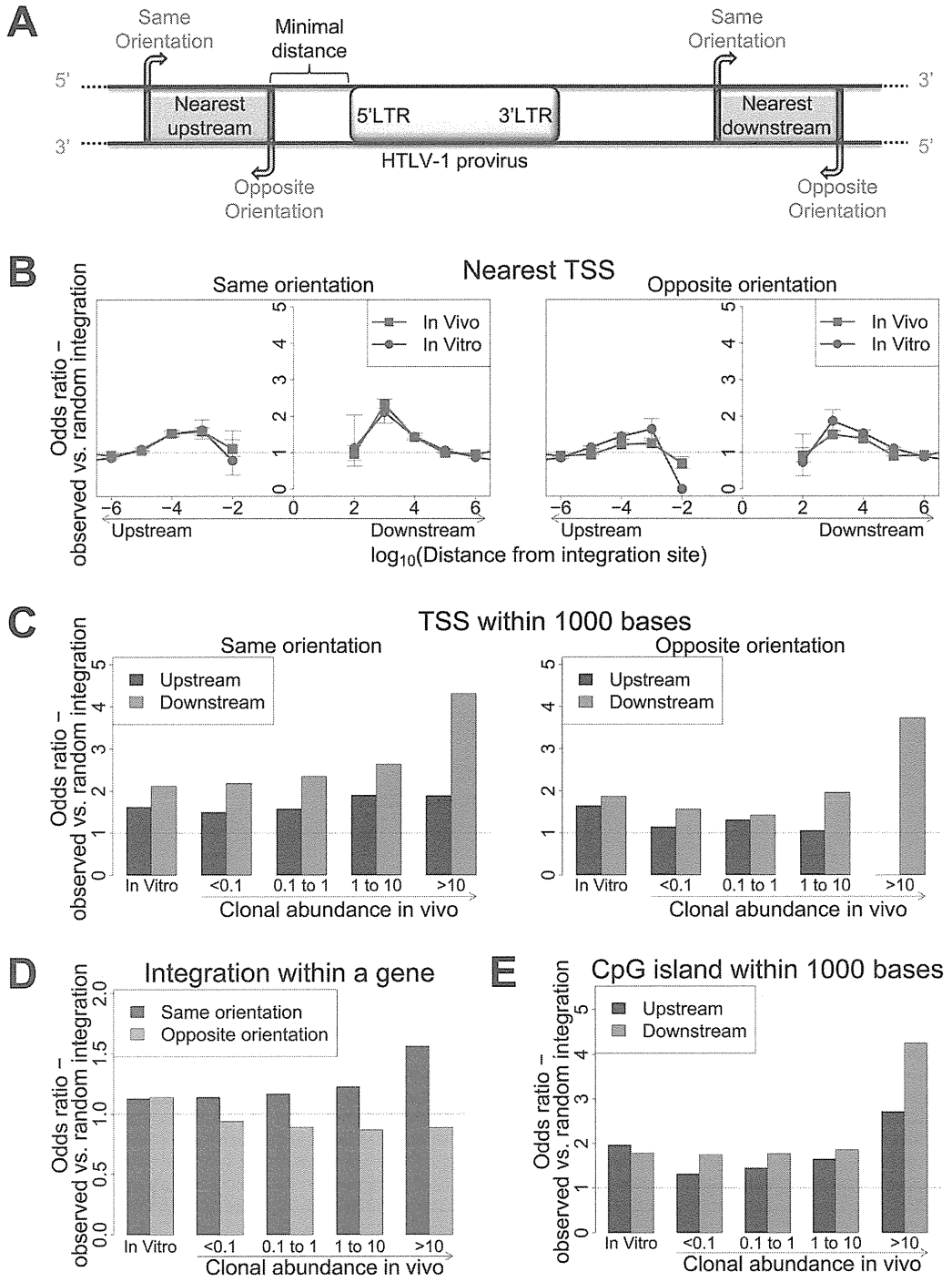

Figure 1. Genomic environment at HTLV-1 proviral integration site determines integration in vitro and abundance in vivo. (A) Blue blocks denote a genomic feature such as a transcription start site. The distance to the nearest genomic feature is calculated (unless otherwise stated) separately for features upstream (closer to 5′ LTR) and downstream of the provirus. Unless otherwise stated, distance is calculated to the nearest end of the genomic feature. Where the genomic feature has an orientation (i.e. transcription units) its orientation relative to the transcriptional orientation of the provirus is indicated as "same" or "opposite". (B) to (E): proportion of observed integration sites compared to random expectation. (B) Frequency of integration in proximity to transcriptional units (RefSeq). In vitro denotes a combined dataset from two independent experiments (see Table 1). (C) Frequency of integration within 1 kb of a TSS according to clonal abundance (cells in a given clone per 10 000 PBMCs). (D) The excess frequency (compared with random) of observing a provirus within a transcription unit was greater among abundant clones in vivo integrated in the same transcriptional orientation (blue) but not in opposite orientation (orange). (E) The excess frequency (compared with random) of observing a provirus within 1 kb of a host CpG island increased with increasing clonal abundance, in particular where the CpG island lay downstream of the integration site.

doi:10.1371/journal.ppat.1003271.g001

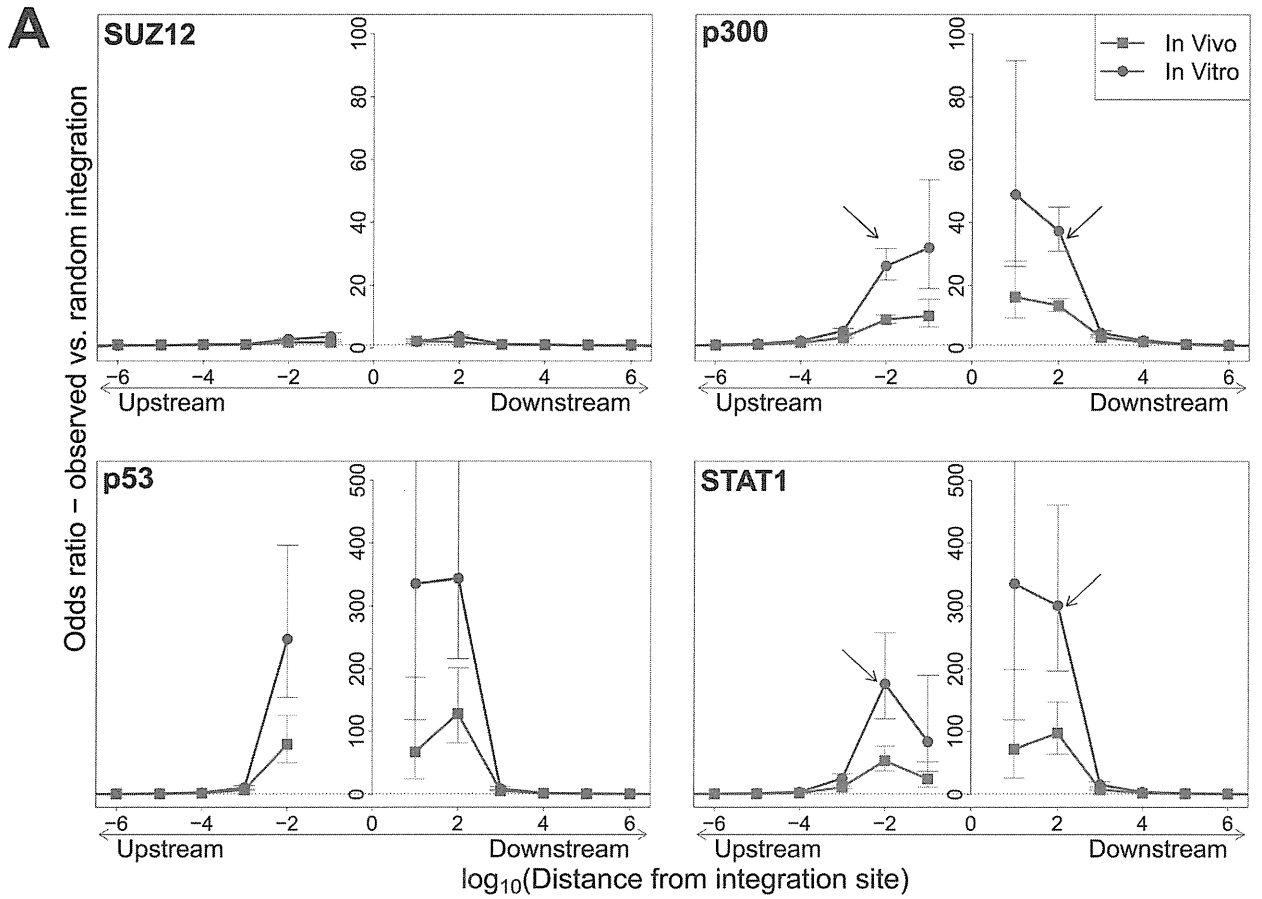

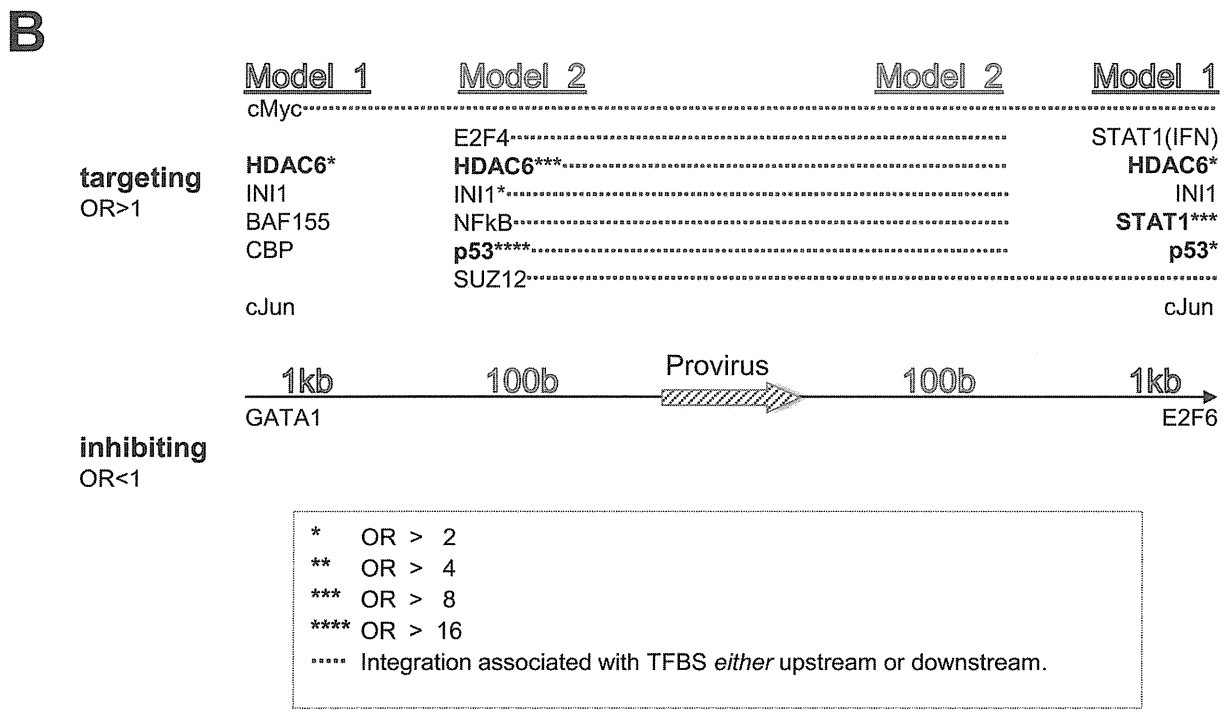

Figure 2. Influence of host TFBS on integration site targeting. (A) Bias in integration in proximity to TFBS (based on ChIP-seq experiments), measured by the odds ratio compared to random expectation. Four representative plots are shown; see also supplementary information. The excess frequency of integration in proximity to TFBS was frequently greater in in vitro infection than in clones isolated from PBMCs in vivo, and greater in low abundance clones in vivo than high abundance clones in vivo (see bottom right panel and supplementary information). Arrows indicate a

symmetrical (p300) or asymmetrical (STAT1) bias towards integration in proximity to TFBS, as well as a lower bias in close proximity to IS (STAT1). See also supplementary Table S4 for underlying data. (B) TFBS independently associated with integration frequency in vitro were identified by multivariate analysis. OR – odds ratio. TFBS shown above the line were associated with an excess frequency of integration compared with random (OR>1); TFBS below the line were significantly less likely to lie near the provirus (OR<1). Model 1 and Model 2 (carried out independently) test for TFBS within 1 kb and 100 bp of IS, respectively.
doi:10.1371/journal.ppat.1003271.g002

Integration sites observed in vivo showed a similar bias towards proximity to TFBS, with two important differences. First, the OR was in each case lower than that observed in in vitro integration. Second, the magnitude of the bias (OR) declined as clonal abundance increased (Figure 3; supplementary Figure S3).

Effect of HTLV-1 integration site on Tax expression

We wished to identify features of the genomic integration site that favour expression of the HTLV-1 provirus. We hypothesized that the genomic environment flanking the proviral integration site determines the rate of spontaneous expression of the HTLV-1 transactivator protein Tax by a given infected T-cell clone: that is, the proportion of cells in that clone that express Tax within a given time interval. $CD8^+$ T-cells were depleted from fresh unstimulated PBMCs of 10 infected HAM/TSP patients (to preclude CTL-mediated lysis), and the $CD8^-$ population was incubated in vitro overnight to allow spontaneous expression of the Tax protein [15]. We then sorted the cells by flow cytometry to isolate Tax^+ and Tax^- cells and analysed the integration sites in the two cell fractions.

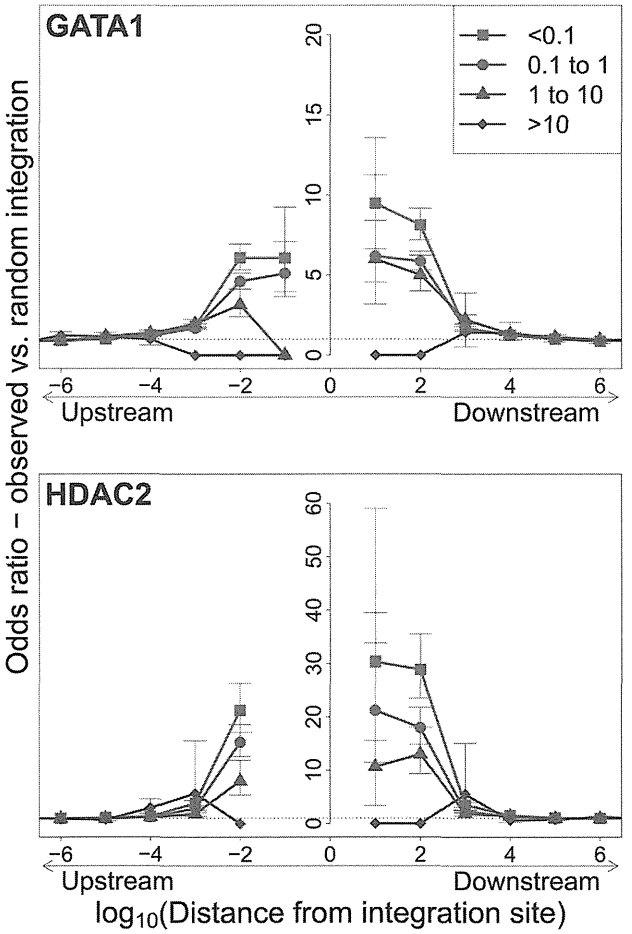

Figure 3. Influence of host TFBS on clonal abundance. Bias in integration in proximity to TFBS (based on ChIP-seq experiments), measured by the odds ratio compared to random expectation. Two representative plots are shown; see also supplementary Figure S3. The excess frequency of integration in proximity to TFBS was greater in low abundance clones in vivo than high abundance clones in vivo. See also supplementary Table S5 for underlying data.
doi:10.1371/journal.ppat.1003271.g003

We measured the proportion of each clone that spontaneously expressed Tax by quantifying individual integration sites in the Tax^+ and Tax^- cells, (Figure 4E, and supplementary Figure S7). The observed proportion of Tax^+ cells per clone varied between 0% and 100%. The majority of clones, regardless of clonal abundance, were either >90% Tax^+ or >90% Tax^-. This observation is consistent with the hypothesis that the rate of spontaneous expression of Tax is an intrinsic property of each clone and is determined by the proviral integration site.

When the provirus was integrated within a host gene, we observed a slight but significant excess frequency of Tax^+ cells compared with Tax^- cells (46% vs 43% respectively, $p<10^{-3}$, χ^2 test). However, while the proviruses in the Tax^+ cells were found with equal frequency in the same or the opposite transcriptional orientation to the host gene in which they were integrated, the Tax^- cells were significantly more frequently present in the same orientation as the host gene (52% of Tax^+ vs 59% of Tax^- cells, $p<10^{-15}$, χ^2 test). Thus, T cell clones that were 100% Tax^- were significantly more likely to carry a provirus in the same orientation as the host gene (Figure 4B).

The relative position (upstream or downstream of the integration site) and the transcriptional orientation of the nearest host gene influenced not only the clonal abundance (Figure 1) but also spontaneous Tax expression. Where the nearest host gene lay in the same transcriptional orientation as the HTLV-1 provirus, the presence of a host TSS (Figure 4A) or CpG island (Figure 4C) within 1 kb upstream of the provirus was associated with silencing of Tax, whereas a TSS or CpG island within 1 kb downstream was associated with Tax expression. The closer the upstream gene was to the integration site, the lower was the proportion of Tax^+ cells if the gene was in the same orientation (Figure 4D). In contrast, where the nearest host gene was in opposite transcriptional orientation, this asymmetrical effect of the nearby host gene was not observed (Figure 4A, right-hand panel; Figure 4D).

The mean proportion of Tax^+ cells in one clone (across all clone abundance classes) was 60%. We wished to test whether proximity to TFBS would alter this proportion. We found that the presence of certain TFBS (including STAT1, cJun, NRSF) within 1 kb upstream of the integration site was associated with a higher proportion of Tax^+ cells in the respective T-cell clone (Figure 5A). A notable exception was BRG-1, which showed a strong opposite asymmetric effect: cells containing a BRG-1 site just upstream of the provirus were more likely to be Tax^-, whereas cells with a BRG-1 site just downstream of the provirus were more likely to be Tax^+ (Figure 5A, top left panel).

To identify the TFBS that were independently and significantly associated with spontaneous Tax expression, a logistic regression analysis was carried out as described above (Figure 2B) for integration site targeting. The results (Figure 5B, see also supplementary Table S7) confirmed the asymmetric effects of the BRG-1 binding site, and in addition revealed significant

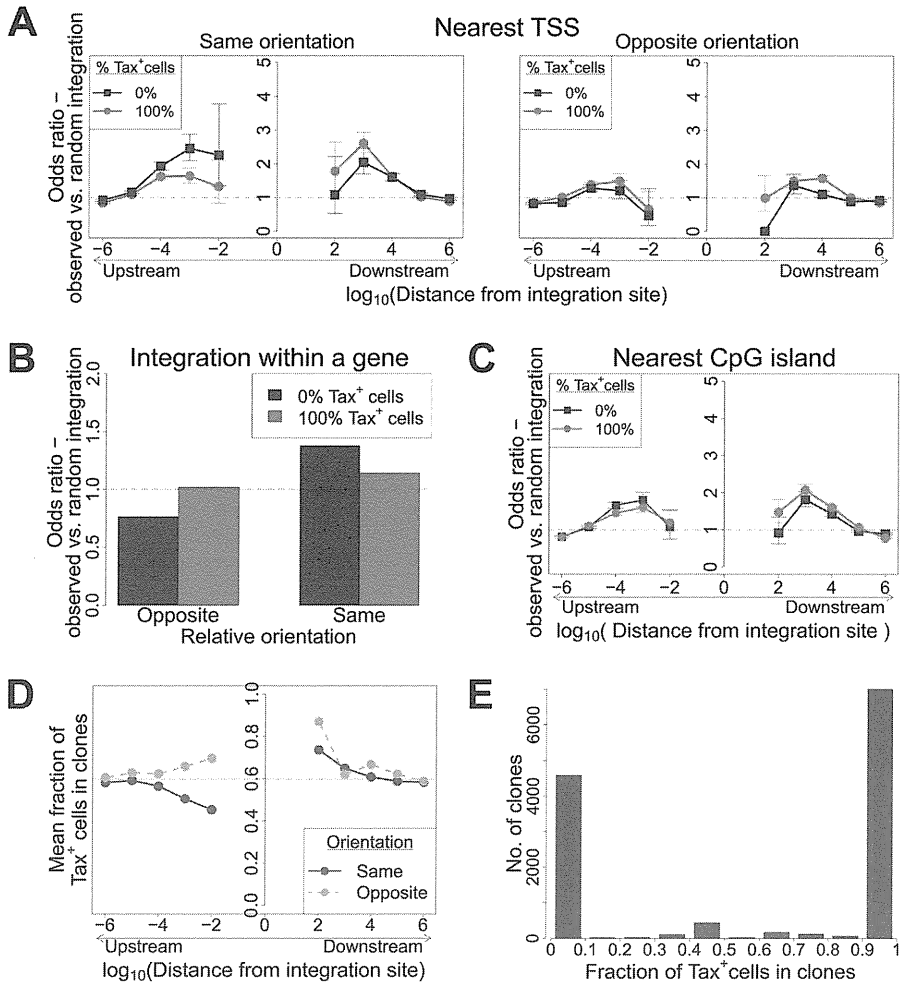

Figure 4. Genomic environment at HTLV-1 proviral integration site associated with proviral expression after 18 h in culture. CD8-depleted PBMCs were placed in culture overnight and sorted by flow cytometry to isolate Tax^+ and Tax^- cells, followed by integration site analysis of sorted cells. (A)–(C): proportion of observed integration sites compared to random expectation. (A) Frequency of integration in proximity to transcriptional units (RefSeq) in clones that were 100% Tax^+ or 100% Tax^-, according to the relative transcriptional orientation of the provirus and the host gene. The peak of integration at 1 kb mirrors that observed in vivo in unsorted cells (Figure 1B). However, the integration site in Tax^- clones was more likely than in Tax^+ clones to possess a nearby upstream TSS in the same orientation, and less likely to lie nearby a downstream TSS in the same orientation (or any relative position in the opposite orientation). (B) The provirus in Tax^- clones (blue) was oriented in the same transcriptional sense as the host gene in which it was integrated more frequently than random. The orientation of Tax^+ clones (pink) did not differ from random. (C) Frequency of integration in proximity to CpG islands in clones that were 100% Tax^+ or 100% Tax^-. The peak of integration at 1 kb mirrors that observed in vivo in unsorted cells and in vitro (Figure S4). (D) Mean fraction of Tax^+ cells in clones with a TSS at a given distance (log scale) from the integration site, according to the relative transcriptional orientation of the provirus and the host TSS. The dotted line denotes the mean fraction of Tax^+ cells across all clones. (E) Frequency distribution of clones according to the frequency of Tax^+ cells in the respective clones. See supplementary Figure S7 for detailed frequency distribution separated according to clone abundance.
doi:10.1371/journal.ppat.1003271.g004

asymmetric associations between Tax expression and several other TFBS, notably STAT1, NRSF, and HDAC1. Thus, a STAT1 binding site 100 bp upstream of the provirus strongly favoured Tax expression, but the presence of a downstream STAT1 binding site was not an independent predictor of Tax expression after multivariate analysis. Conversely, an NRSF binding site 100 bp downstream was a significant predictor of Tax negativity, but the closest upstream NRSF binding site was not independently associated with Tax expression. The asymmetry of these associations contrasts with the predominantly symmetrical associations observed between TFBS and integration site targeting (Figure 2B), and suggests a mechanistic interaction between transcription of the provirus and transcription of the flanking host genome.

Tax^+ cells are more frequent in low-abundance clones

To test the hypothesis that the level of Tax expression is correlated with the in vivo abundance of the infected T cell clone, we divided all detected clones into four abundance bins based on the total number of cells observed in each clone. There was a significant negative correlation between clone abundance and the proportion of Tax^+ cells in the respective abundance bin (Figure 5). That is, small clones were more likely to be Tax^+, and this likelihood decreased as clone abundance increased. We conclude that, at least in cells from HAM/TSP patients, the majority of spontaneous Tax expression observed is due to the large number of low-abundance clones, rather than a small number of high-abundance clones.

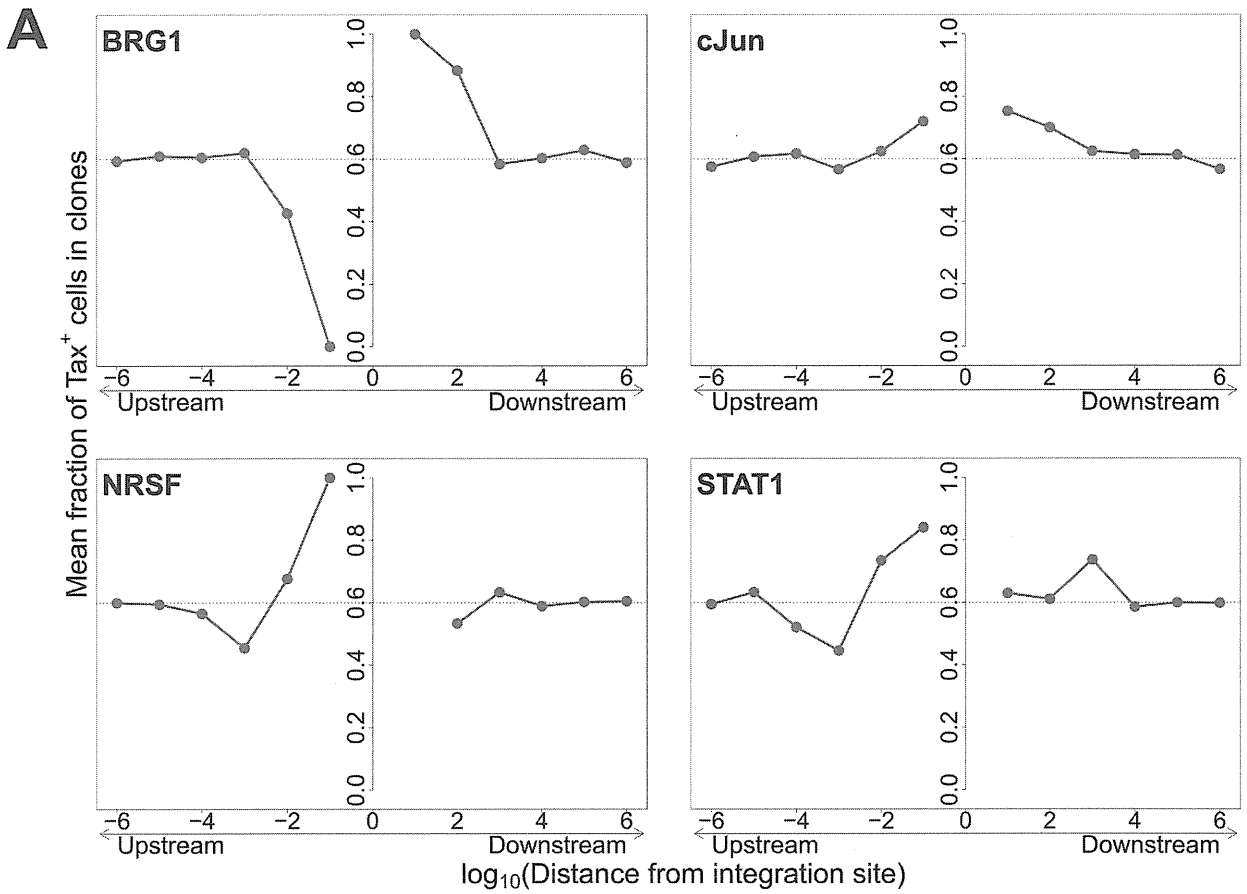

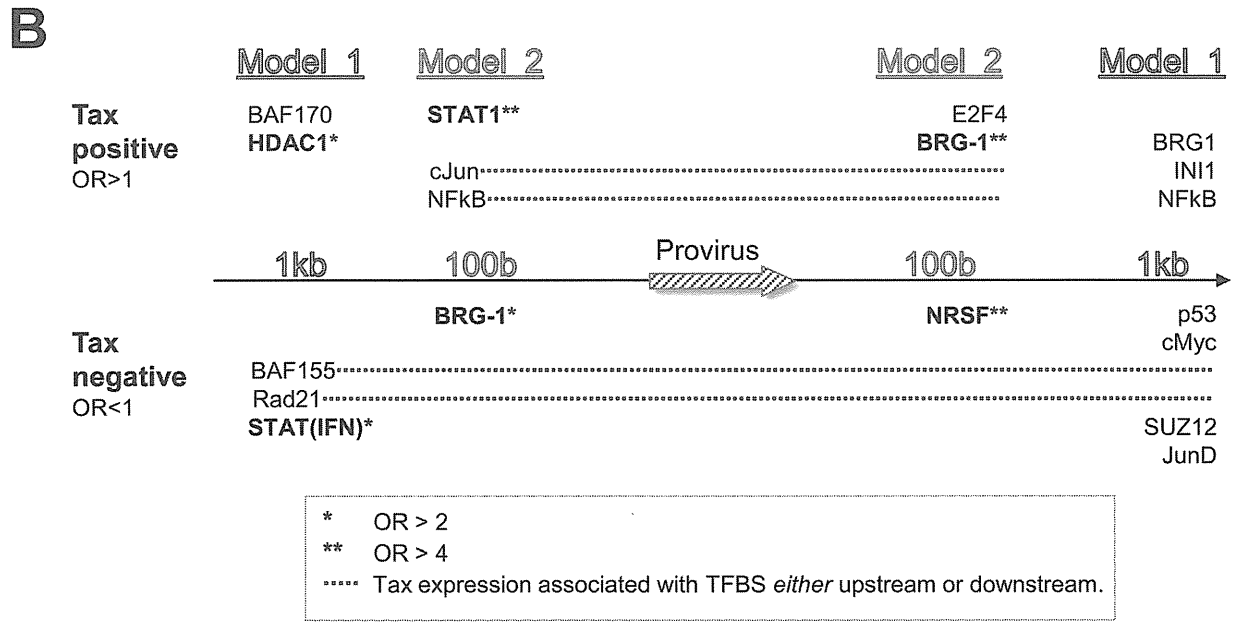

Figure 5. Influence of proximity to TFBS on Tax expression. (A) Mean fraction of Tax$^+$ cells in clones with a TFBS (based on ChIP-seq experiments) at a given distance from the IS. Four representative plots are shown. (B) TFBS that were independently associated with Tax expression were identified by multivariate analysis, outcome measure . TFBS shown above the line were associated with Tax expression (OR>1); TFBS below the line were associated with Tax silencing (OR<1). Model 1 and Model 2 (carried out independently) test for TFBS within 1 kb and 100 bp of IS, respectively.

doi:10.1371/journal.ppat.1003271.g005

Discussion

An understanding of the regulation of proviral latency is required for attempts to eradicate latent retroviruses and to optimize retroviral vectors for in vitro and in vivo use. In HIV-1 infection, a reservoir of latently infected cells persists indefinitely in the face of antiretroviral drug therapy and precludes eradication of the infection (reviewed in [23]). In HTLV-1 infection, proviral expression is difficult to detect in fresh PBMCs: however, the strong, chronically activated host immune response and the selective oligoclonal proliferation of HTLV-1-infected T cells argue that the virus is continuously or intermittently expressed in vivo [4,24].

The abundance of an HTLV-1-infected T cell clone in vivo will be determined by the net effect of two main selection forces: its ability to proliferate and its susceptibility to killing by the strong CTL response [4]. If these forces acted upon all clones equally, the clones would have the same relative abundance in the host. However, Gillet et al [11] showed a wide variation in clone abundance both within and between infected individuals and over time. We hypothesized that this variation between clones is caused by the genomic environment of the integrated provirus, by determining the frequency and intensity of expression of proviral genes, in particular Tax and HBZ, which in turn promote cell proliferation and thereby confer a selective advantage on the infected T cell clone.

To identify the host genomic factors that determine integration site targeting, we mapped and quantified proviral integration sites isolated from two independent in vitro infection experiments. We assume that the pattern of integration observed in short-term in vitro infection reflects the initial pattern of integration in vivo, before the selection exerted during chronic infection. The results confirmed our previous observations [10,11] that the virus is targeted to transcriptionally active regions of the genome, within or near to a host gene. There was no bias in the orientation of the provirus in the initial infection, indicating that the bias observed in integration sites isolated from PBMCs is a result of the long-term selection forces acting on the infected clones in vivo.

We observed a bias towards integration in proximity to particular transcription factor binding sites. This bias was remarkably strong in certain cases (STAT1, NRSF) in single-factor analysis. Because clusters of different TFBS are frequent in the genome [22], we carried out a multivariate (logistic regression) analysis to identify the TFBS that were independently and significantly associated with an excess frequency of integration. The results (Figure 2B) confirmed the identification of p53, HDAC6 and STAT1 as significant independent correlates of integration. Further independent predictors of integration included Ini1 (see below), cMyc, cJun and NF-kB (Figure 2B). p53 and STAT1 both play important roles in HTLV-1 infection. HTLV-1 dysregulates p53 signalling pathways in vivo [25]; it is not known whether insertional mutagenesis contributes to this dysregulation. HTLV-1 also causes widespread activation of interferon-stimulated genes in vivo, including the key transcriptional regulator STAT1 [25]. A strong association was reported between STAT1 and MLV integration [26]; the authors attributed this to an association between MLV integration and particular epigenetic marks (H3K4me3, H3K4me1 and H3K9ac) at the integration site.

The proportion of all integration sites near any one TFBS was in the minority. This observation indicates that proximity to the transcription factor binding site itself is not sufficient for integration, but suggests that these transcription factors (or an associated host factor) increase the efficiency of proviral integration. Host factors associated with HIV integrase have been thoroughly studied [27]; the most important is the lens epithelium-derived growth factor (LEDGF/p75, [28]), which determines integrase localization [29] and targeting of HIV integrase to transcription units [21]. A study of host factors associated with HTLV-1 integrase is currently underway.

The observed bias towards integration near certain TFBS was predominantly symmetrical and short-range, reaching a maximum at 100b from the integration site and falling to random expectation at ~10 kb (Figure 2A). In many instances the bias dropped sharply at less than 100b from the integration site: we suggest that this drop is due to steric hindrance between the pre-integration complex and the DNA-bound transcription factor.

In contrast to the symmetry observed in the association between genomic features (such as TFBS) and the frequency of initial integration, we found significant asymmetric interactions between the flanking host genome and the integrated provirus in determining clonal abundance and spontaneous proviral expression. Both the relative position of the nearest host gene (upstream or downstream of the provirus) and its relative transcriptional orientation showed significant associations with clone abundance and expression. Previous studies [1,2] reported contradictory evidence on the role of an upstream same-sense host promoter in either promoting or suppressing proviral transcription. More recently, Shan et al [30] have shown in Bcl-2-transduced $CD4^+$ T cells, infected in vitro with GFP expressing modified HIV, that persistent expression of GFP was associated with opposite sense orientation, while inducible expression was associated with same sense orientation. The evidence obtained here demonstrates that, in natural HTLV-1 infection, the presence of a same-sense host gene promoter upstream of the integrated provirus is associated with inhibition of spontaneous proviral expression, suggesting the operation of transcriptional interference. We conclude that the transcriptional interaction between host and HTLV-1 operates at two levels. First, at a regional level – within 10 kb of the provirus – transcriptional activity of the flanking host genome favours proviral gene expression [10,11], presumably because of accessibility of the euchromatin to transcription complexes. Second, at a local level – within 100b to 1000b – transcriptional interference by a same-sense host promoter within 1 kb upstream can override the regional effect and inhibit proviral transcription.

Two observations reported here demonstrate that proviral integration and expression are not determined simply by the accessibility of chromatin. First, whereas some TFBS were associated with HTLV-1 proviral integration more frequently than expected, the frequency of other TFBS showed no such bias. Second, the asymmetric associations observed between proviral orientation and position with respect to flanking host genes and the abundance and expression of the HTLV-1 provirus argue for a mechanistic interaction between transcription of the HTLV-1 provirus and transcription of the flanking host genome.

An observation of particular interest is the opposing effect of a BRG-1 binding site upstream and downstream of the provirus (Figure 5A). BRG-1, one of the two ATPase components required for the activity of the SWI/SNF complex [31], controls gene expression by remodelling chromatin, i.e. by repositioning nucleosomes to control the access of transcriptional complexes to the DNA. BRG-1 can cause both gene repression [32] and gene activation [33]; the balance appears to depend on which other subunits are recruited to the SWI/SNF complex [34]. Easley et al [35] found that BRG-1 is required for Tax expression and HTLV-1 replication in vitro, and Rafati et al [36] found that the BAF subclass of the SWI/SNF complex repressed HIV-1 transcription whereas the PBAF subclass promoted transcription. Our observation (Figure 5A) that a BRG-1 site upstream of the provirus is

associated with silencing of Tax, while a BRG-1 site downstream is associated with Tax expression, is consistent with our conclusion (above) that transcriptional interference dominates the transcriptional interaction between the provirus and the flanking host genome.

The Ini1 subunit of SWI/SNF interacts directly with HIV-1 integrase [37]; a fraction of Ini1 moves transiently to the cytoplasm to associate with the HIV-1 preintegration complex [38]. However, the function of Ini1 in HIV-1 proviral integration and expression in vivo is not understood. We found that genomic sites for Ini1 binding were significantly associated with HTLV-1 proviral integration (Figure 2B). The presence of an Ini1 site 1 kb downstream of the provirus was associated with spontaneous Tax expression, similar to the effect of the downstream BRG-1 site. Finally, the SWI/SNF subunit BAF155 was overrepresented 1 kb upstream of the integration site (Figure 2B), and was associated with Tax silencing when present either upstream or downstream of the provirus (Figure 5B).

The HTLV-1 Tax protein acts in concert with host cell transcription factors (notably CBP/p300) on the promoter/enhancer in the viral 5′ LTR, driving plus-strand transcription in a strong positive feedback loop. Tax also acts on response elements for NF-kB, CREB and the serum response factor (SRE) to upregulate expression of a wide range of host genes [39]. Finally, Tax promotes cell cycle progression by accelerating passage through G1 and inhibiting the G1/S and G2/M checkpoints [40]. The net effect of Tax expression is therefore to drive activation and proliferation of the infected T cell. We previously reported that spontaneous Tax expression in fresh unstimulated PBMCs was associated with proliferation of the respective cell in vivo [41]. We therefore expected to observe a positive correlation between the frequency of spontaneous Tax expression by a given clone ex vivo and the abundance of that clone in vivo. However, the results obtained here (Figure 6) demonstrate the opposite, i.e. a highly significant negative correlation. This correlation is likely to be caused by the strong host immune response to the virus. The Tax protein is highly immunodominant in the class 1 MHC-restricted cytotoxic T lymphocyte (CTL) response to HTLV-1 [14,42], and the *tax* gene is frequently silenced in vivo by mutation or epigenetic changes such as DNA methylation in both untransformed and malignantly transformed (leukemic) cells [43]. Cells that express a high level of Tax are killed by CTLs faster than low Tax-expressing cells [44]. Therefore, suppression or loss of Tax expression may confer a survival advantage on the infected clone in vivo. We conclude that the small (low-abundance) HTLV-1-infected clones express Tax at a higher rate and turn over faster in vivo than the high-abundance clones. It is possible that the critical role of Tax in the HTLV-1 lifecycle is not to maintain clone abundance but rather to promote virion production and infection of new cells by cell contact via the virological synapse [45,46].

The negative correlation observed between clone abundance and the percentage of Tax^+ cells, although it was highly significant in all patients combined, was not uniform in every patient. In a small number of patients (in particular those with a high oligoclonality index, Supplementary Figure S8), the most abundant clones (bin 4, clones with greater than 10 cells) contained a high proportion of Tax^+ cells, suggesting that certain antigen-expressing clones escaped control by the immune response, for example by CTL escape mutations in the *tax* gene [47]. However, clone-specific sequencing of exon 3 of the *tax* gene of 38 clones (>10 cells) from 8 patients did not reveal significant differences in the occurrence of Tax mutations between clones with a high or low frequency of Tax^+ cells; and only in one patient was a difference in amino acid sequence found between one clone and the others (data not shown).

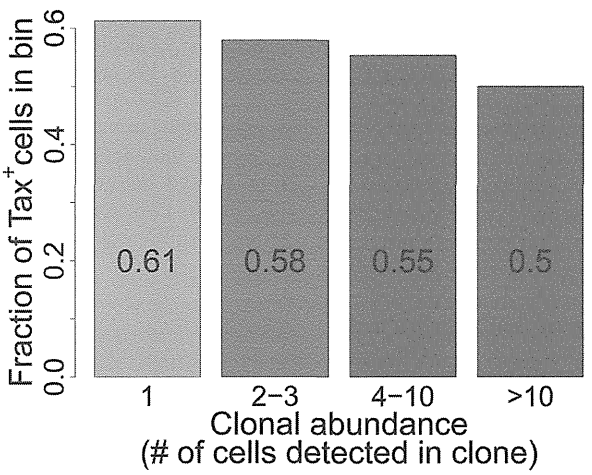

Figure 6. Tax^+ cells are more frequent in smaller clones. Mean fraction of Tax^+ cells in bins of increasing clonal abundance (total number of cells in each respective clone). The fraction of Tax^+ cells was negatively correlated with clonal abundance ($p<10^{-16}$, χ^2 test for trend).
doi:10.1371/journal.ppat.1003271.g006

Interestingly, while Tax^+ cells were more frequent in low-abundance clones, certain features favouring proviral expression (e.g. a downstream host TSS) also favoured clonal expansion. The association between clonal abundance and proviral integration within 1 kb of a downstream host TSS was maintained even within Tax^- clones, consistent with the idea that the selective expansion of these clones is driven by other proviral genes.

These observations raise the possibility that the equilibrium abundance of an HTLV-1-infected T cell clone in vivo is determined not by Tax but by the HBZ gene, encoded on the negative strand of the provirus. Satou et al showed that *HBZ* mRNA promoted proliferation of the infected cell, and whereas Tax expression is frequently undetectable, HBZ appears to be persistently expressed in fresh cells isolated from both non-malignant cases of HTLV-1 infection and cases of adult T-cell leukemia/lymphoma [16]. Further, Macnamara et al recently showed that the CTL response to HBZ is a critical determinant of the equilibrium proviral load in vivo [17]

In this study we examined Tax expression only among $CD4^+$ T cells. A small percentage of infected cells are $CD8^+$ T cells [48,49]; it is possible that the genomic factors that determine targeting and expression of HTLV-1 differ in $CD8^+$ cells. Also, the propensity of a cell to express Tax was measured by quantifying the frequency of spontaneous Tax expression after 18 hours incubation in vitro. Two lines of evidence suggest that this measure is relevant to HTLV-1 infection and pathogenesis in vivo. First, cells which express Tax ex vivo turn over faster in vivo [41]. Second, the proportion of $CD4^+$ cells that express Tax after overnight culture is significantly associated with the HTLV-1 inflammatory disease HAM/TSP [50]. The individuals studied here were all patients with HAM/TSP: the mean level of spontaneous Tax expression is lower in asymptomatic HTLV-1 carriers, but it is unlikely that the molecular mechanisms that govern proviral latency differ qualitatively between asymptomatic carriers and patients with HAM/TSP.

It will be important to compare the present results with the genomic factors associated with HBZ expression or silencing. At

present this cannot be done by flow-sorting because existing HBZ-specific antibodies are insufficiently sensitive to detect the low expression levels of HBZ protein in primary cells. We are currently testing the hypothesis that Tax-specific and HBZ-specific CTL clones selectively lyse different clonal populations in vitro.

We have identified host genomic factors that determine the integration site, the proviral expression and selective clonal expansion of HTLV-1 in natural infection in vivo: these factors are summarized in Figure 7. These results open the way to test the molecular mechanisms involved.

Materials and Methods

Ethics statement

Blood samples were donated by HTLV-1-infected individuals attending the HTLV-1 clinic at the National Centre for Human Retrovirology (Imperial College Healthcare NHS trust) at St Mary's Hospital, London UK, with fully informed written consent. This study was approved by the UK National Research Ethics Service (NRES reference 09/H0606/106).

DNA samples (Table 1)

PBMCs were isolated using Histopaque-1077 (Sigma-Aldrich) and cryopreserved in FBS (Gibco) containing 10% DMSO (Sigma-Aldrich). DNA extraction was carried out using the DNeasy Blood & Tissue kit (Qiagen) according to the manufacturer's protocol.

Table 1. IS datasets used.

Dataset	total IS	total infected individuals	reference
in vitro (1)	4521	N/A	[11]
in vitro (2)	1805	N/A	This publication
In vivo (1)	78563[1]	63	[11]
In vivo (2)	20202	10	This publication
Tax Negative	6700	10 (pooled)	This publication
Tax Positive	13054	10 (pooled)	This publication
Random UIS	176505	N/A	This publication

[1]For the purpose of this work, only one time point was used for each patient (most recent available if multiple time points were originally analysed).
doi:10.1371/journal.ppat.1003271.t001

In vitro infection

In vitro infection was carried out in two independent assays as previously described [11]. Jurkat (JKT) cells were co-cultured for 3 h with γ-irradiated (^{137}Cs, 40,000 cGy) MT2 cells [51], labelled with anti-CD4 MicroBeads (Miltenyi). MT2 cells were then depleted from the co-culture using magnetic separation (Miltenyi), and infected JKT cells were maintained in culture for 14 days in RPMI (supplemented by L-glutamine, penicillin, streptomycin) containing 10% FBS for 18 hours at 37C with 5% CO_2. Genomic

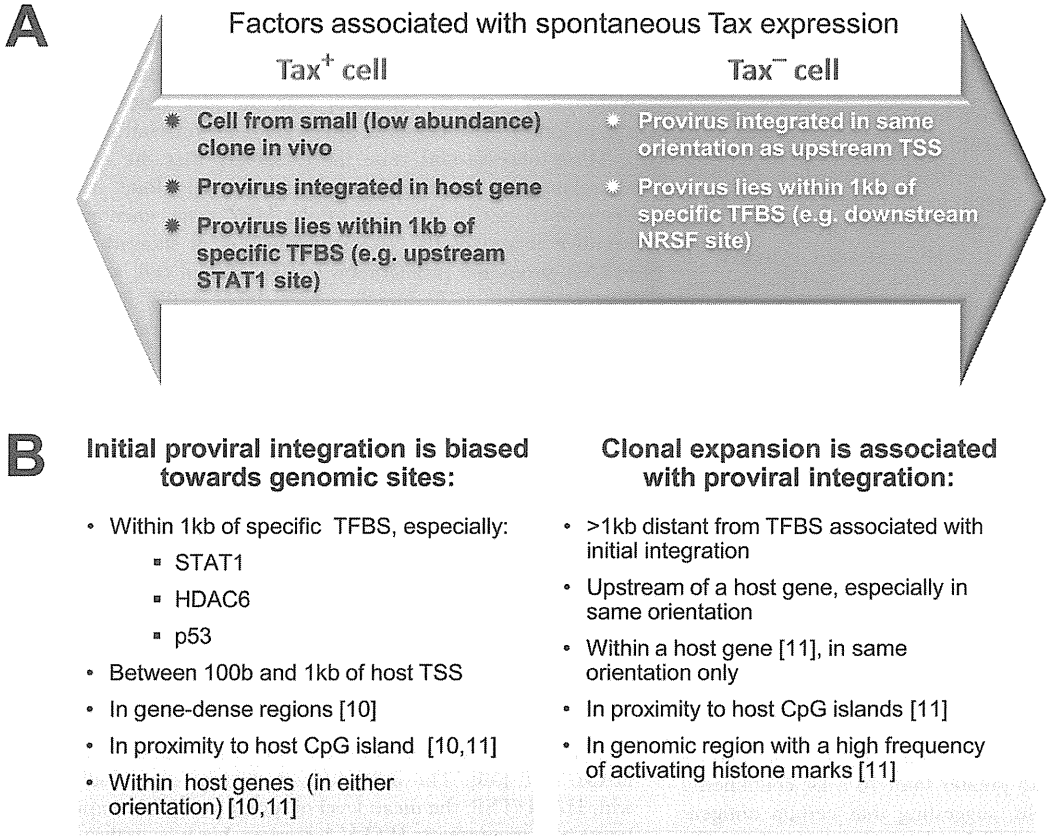

Figure 7. Genomic correlates of HTLV-1 proviral targeting, clonal expansion and proviral expression. (A) Factors associated with the presence or absence of spontaneous Tax expression by a given cell after short-term (18 h) in vitro incubation. (B) Features of the genomic environment of the provirus associated either with initial integration (left panel), or clonal expansion in vivo (right panel). Findings were made in the present study unless otherwise stated. TSS – transcription start site. TFBS – transcription factor binding site.
doi:10.1371/journal.ppat.1003271.g007

DNA was extracted and the proviral integration sites (IS) analysed as previously described [11]. IS from MT2 were also analysed to exclude possible contamination of the JKT IS. No contaminating MT2 IS were found after 14 days.

Tax sorting

See also supplementary Figure S5, supplementary Table S6. PBMCs from 10 patients with HAM/TSP with a high proviral load (range 12.2–50.6 copies per 100 PBMC) were depleted of $CD8^+$ cells using magnetic depletion (Miltenyi) and incubated in RPMI (supplemented by L-glutamine, penicillin, streptomycin) containing 10% FBS for 18 hours at 37C with 5% CO_2. After 18 h culture, the cells were stained for intracellular expression of Tax (anti-Tax mAb LT4) and sorted using FACS (FACSAria IIIU, BD Biosciences) to isolate two populations of live $CD4^+$ cells based on Tax expression. Gates were set (FACSDiva, BD Biosciences) to ensure a clear demarcation between the Tax^+ and Tax^- populations (Figure S6). DNA was extracted from whole unsorted PBMCs from each patient and analysed separately to identify the patient of origin of each clone; 46% of the clones were attributed in this way. To calculate the fraction of Tax^+ cells in a given clone, the frequency of Tax^+ and Tax^- cells were normalized to the mass of genomic DNA per cell from each respective cell population, to correct for experimental variation in efficiency of genomic DNA isolation (Table S6),

Analysis of IS

Identification and quantification of proviral integration sites was done as previously described [11]. HTLV-1 infected DNA was randomly sheared by sonication (Covaris S2) and then blunt-ended (Klenow polymerase) and ligated to a partly double-stranded DNA linker. Following a nested PCR step, the resulting DNA libraries were deep sequenced using the Illumina GA-II platform. DNA sequence was aligned to the human genome reference (UCSC hg18, excluding haplotype and "random" sequences) using the ELAND algorithm. Distinct IS were grouped based on integration site and quantified based on number of distinct shear sites isolated and the respective patient's proviral load.

DNA sequences from ~190000 random sites in the human genome (hg18) were generated using Galaxy [52,53,54] and back-aligned to the human genome using the same pipeline to eliminate any potential bias due to alignment limitations.

Calculation of clonal abundance

The absolute abundance of a given clone was defined as the number of proviral copies of that clone per 10^4 PBMCs. Given n_i - the number of proviral copies for the i^{th} clone, and S – the total number of clones identified in the sample, the absolute abundance was calculated for PBMC samples according to the following formula:

$$\text{absolute abundance} = \text{PVL} \times \frac{n_i}{\sum_{i=1}^{S} n_i}$$

Clone abundance bins were defined on a logarithmic scale since proviral load (used in calculation of abundance) follows a logarithmic distribution [55]. The number of clones in each clone abundance bin is given in Table S1. For samples sorted for Tax protein expression, where proviral load data were not available, the clonal abundance bins were set according to proviral copy count.

Bioinformatic analysis of genomic environment

Transcription units and CpG island data were retrieved from the NCBI (ftp.ncbi.nih.gov/gene/) and UCSC tables [56], respectively. Annotations to the human genome were obtained from published datasets (Table S3) including ChIP-seq experiments on primary $CD4^+$ T cells where available; otherwise, data on human $CD4^+$ T cell lines or other human cell lines were used. We used the SISSRs algorithm [57] to identify the position of a putative transcription factor binding site in published ChIP-seq data where raw ChIP-seq data were available.

Annotations positions were compared to the IS using the R package hiAnnotator (http://malnirav.github.com/hiAnnotator), kindly provided by N. Malani and F. Bushman (University of Pennsylvania, USA).

Statistical analysis

Statistical analysis was carried out using R version 2.13.0 (http://www.R-project.org/). Two separate logistic regression analyses were carried out, respectively, to identify independent predictors of HTLV-1 integration targeting and independent predictors of Tax positivity. Genomic annotations used to derive input variable were published ChIP-seq datasets (see Bioinformatic analysis above; Table S3). For integration targeting, the binary outcome measure was a "true" integration site (from 4521 identified in vitro integration sites) or a "false" integration site (45210 random genomic locations). For spontaneous Tax expression, the binary outcome was Tax positivity (20813 Tax^+ cells) or Tax negativity (10326 Tax^- cells). Each TFBS was tested (presence or absence of the TFBS within a given distance of the integration site) as an independent predictor in each analysis. For each outcome variable, two separate analyses were carried out, respectively at two distances of the integration site - 100 bases and 1 kb.

First, for each TFBS and at each distance, we tested whether the relative position (upstream/downstream) of the integration site and the TFBS determined the outcome by using a likelihood ratio test to compare two competing models: 1) presence or absence of TFBS upstream or (separately) downstream; 2) presence or absence of TFBS, regardless of relative position. Next, we carried out univariate analysis of each individual TFBS, based on the model chosen by the likelihood ratio test. Only TFBS that were significant (p-value$<$0.05) after correction for multiple comparisons (Benjamini-Hochberg) were used in the multivariate analysis. Multivariate analysis was carried out using a step-down logistic regression method.

Supporting Information

Figure S1 Influence of host TFBS on integration site targeting – in vitro. Bias in integration in proximity to TFBS (based on ChIP-seq experiments), measured by the odds ratio compared to random expectation. The bias was maintained across separate datasets, generated by independent in vitro experiments. Dotted line denotes random expectation (OR = 1).
(TIF)

Figure S2 Influence of host TFBS on integration site targeting – in vivo. Bias in integration in proximity to TFBS (based on ChIP-seq experiments), measured by the odds ratio compared to random expectation. The pattern of bias was maintained between different patient clinical groups. Dotted line denotes random expectation (OR = 1). ATLL = Adult T-cell leukaemia/lymphoma . HAM/TSP = HTLV-1 associated myelopathy/Tropical spastic paraparesis. AC = Asymptomatic carrier.
(TIF)

Figure S3 Influence of host TFBS on clonal abundance in vivo. Bias in frequency of integration in proximity to TFBS (based on ChIP-seq experiments), measured by the odds ratio compared to random expectation. TFBS that were associated with integration targeting showed a stronger bias (higher OR) in the clones least expanded in vivo. Clonal abundance is expressed as the number of cells in given clone per 10^4 PBMCs. Dotted line denotes random expectation (OR = 1).
(TIF)

Figure S4 The genomic environment at the HTLV-1 proviral integration site determines integration targeting in vitro and clonal abundance in vivo. Frequency of integration in proximity to CpG islands in clones for in vitro (in blue) and in vivo (purple) integration.
(TIF)

Figure S5 Protocol for flow-sorting of Tax-expressing cells. (A) $CD8^+$ cell-depleted PBMCs were studied from 10 patients with HAM/TSP with a high proviral load. The cells were incubated overnight, fixed and stained for Tax and surface CD4 expression, and sorted on a high-speed flow cytometer (see Figure S6 for details). (B) Recovered cells from all 10 patients were combined in two pools, respectively $CD4^+Tax^+$ cells and $CD4^+Tax^-$ cells. (C) Genomic DNA was extracted from each pool of cells and integration site analysis carried out as described.
(TIF)

Figure S6 Flow cytometry sorting by Tax expression. (A) Representative FACS plots of the gating procedure used (from 1 of 10 samples studied). Lower middle panel shows gating of $CD4^+Tax^+$ ('Tax pos') and $CD4^+Tax^-$ ('Tax neg') populations; these gates were set to distinguish unequivocally between Tax^+ and Tax^- populations. (B) Purity testing of Tax^- sorted cells: Tax^+ cells not detected. C) Purity testing of Tax^+ sorted cells: 0.2% were Tax^-.
(TIF)

Figure S7 Majority of HTLV-1-infected clones were either 100% Tax^+ or 0% Tax^+. Frequency distribution of clones according to the frequency of Tax^+ cells in each respective clone, binned according to number of sister cells detected in sample: bin 1: 1 cell detected; bin 2: 2 or 3 cells detected; bin 3: 4 to 10 cells detected; bin 4: over 10 cells detected.
(TIF)

Figure S8 Tax^+ cells were more frequent in smaller clones. Mean fraction of Tax^+ cells within each bin, in bins of increasing clonal abundance (total number of cells in each respective clone). In the majority of patients there was an inverse correlation between clone abundance bin and fraction of Tax^+ cells: this correlation was highly significant in all patients combined ($P<10^{-32}$). However in certain patients (particularly those with a high oligoclonality Index) the most abundant clones contained a high proportion of Tax^+ cells. Clone abundance bins were defined as in Figure S7.
(TIF)

Table S1 In vivo integration sites – sample data by clone abundance.
(DOC)

Table S2 In vivo integration sites – sample data by patient code.
(DOC)

Table S3 List of annotations datasets used.
(DOC)

Table S4 Odds ratio and clone counts data for a selection of TFBS – in vitro, in vivo vs. random sites.
(XLS)

Table S5 Odds ratio and clone counts data for a selection of TFBS – clonal abundance bins vs. random sites.
(XLS)

Table S6 Tax sorting experiment – sample data.
(DOC)

Table S7 Multivariate analysis results – detailed odds ratios and confidence intervals.
(XLS)

Acknowledgments

We thank Nirav Malani and Frederic D. Bushman at the department of Microbiology, University of Pennsylvania, Philadelphia, PA, USA for the list of random integration sites and for developing software packages; and Laurence Game, Nathalie Lambie and Adam Giess of the Genomics Laboratory at the MRC Clinical Sciences Centre, Hammersmith Hospital, London UK and Robert Sampson at the flow cytometry facility at St Mary's Campus, Imperial College, London UK. Finally we thank Lucy Cook, Heather Niederer and Becca Asquith and her team at the Section of Immunology (Imperial College) for discussions and comments, and the staff and donors at the National Centre for Human Retrovirology (Imperial College Healthcare NHS trust) at St Mary's Hospital, London UK.

Author Contributions

Conceived and designed the experiments: AM GPT CRMB. Performed the experiments: AM NAG. Analyzed the data: AM. Contributed reagents/materials/analysis tools: YT GPT NAG DJL. Wrote the paper: AM CRMB. Clinical diagnosis and assessment: GPT. Designed the statistical analysis: AM DJL CRMB.

References

1. Han Y, Lin YB, An W, Xu J, Yang HC, et al. (2008) Orientation-dependent regulation of integrated HIV-1 expression by host gene transcriptional readthrough. Cell Host Microbe 4: 134–146.
2. Lenasi T, Contreras X, Peterlin BM (2008) Transcriptional interference antagonizes proviral gene expression to promote HIV latency. Cell Host Microbe 4: 123–133.
3. Igakura T, Stinchcombe JC, Goon PK, Taylor GP, Weber JN, et al. (2003) Spread of HTLV-I between lymphocytes by virus-induced polarization of the cytoskeleton. Science 299: 1713–1716.
4. Bangham CR (2009) CTL quality and the control of human retroviral infections. Eur J Immunol 39: 1700–1712.
5. Iwanaga M, Watanabe T, Utsunomiya A, Okayama A, Uchimaru K, et al. (2010) Human T-cell leukemia virus type I (HTLV-1) proviral load and disease progression in asymptomatic HTLV-1 carriers: a nationwide prospective study in Japan. Blood 116: 1211–1219.
6. Matsuzaki T, Nakagawa M, Nagai M, Usuku K, Higuchi I, et al. (2001) HTLV-I proviral load correlates with progression of motor disability in HAM/TSP: analysis of 239 HAM/TSP patients including 64 patients followed up for 10 years. J Neurovirol 7: 228–234.
7. Wattel E, Vartanian JP, Pannetier C, Wain-Hobson S (1995) Clonal expansion of human T-cell leukemia virus type I-infected cells in asymptomatic and symptomatic carriers without malignancy. J Virol 69: 2863–2868.
8. Cook LB, Rowan AG, Melamed A, Taylor GP, Bangham CR (2012) HTLV-1-infected T cells contain a single integrated provirus in natural infection. Blood 120: 3488–3490.
9. Derse D, Crise B, Li Y, Princler G, Lum N, et al. (2007) Human T-cell leukemia virus type 1 integration target sites in the human genome: comparison with those of other retroviruses. J Virol 81: 6731–6741.
10. Meekings KN, Leipzig J, Bushman FD, Taylor GP, Bangham CR (2008) HTLV-1 integration into transcriptionally active genomic regions is associated with proviral expression and with HAM/TSP. PLoS Pathog 4: e1000027.
11. Gillet NA, Malani N, Melamed A, Gormley N, Carter R, et al. (2011) The host genomic environment of the provirus determines the abundance of HTLV-1-infected T-cell clones. Blood 117: 3113–3122.